

JGI Plant Gene Atlas: An updateable transcriptome resource to improve structural annotations and functional gene descriptions across the plant kingdom

Avinash Sreedasyam^{1*}, Christopher Plott¹, Md Shakhawat Hossain^{2#a}, John T. Lovell^{1,3}, Jane Grimwood¹, Jerry W. Jenkins¹, Christopher Daum³, Kerrie Barry³, Joseph Carlson³, Shengqiang Shu³, Jeremy Phillips³, Mojgan Amirebrahimi³, Matthew Zane³, Mei Wang³, David Goodstein³, Fabian B. Haas^{4#b}, Manuel Hiss^{4#c}, Pierre-François Perroud^{4#d}, Sara S. Jawdy⁵, Rongbin Hu⁵, Jenifer Johnson³, Janette Kropat⁶, Sean D. Gallaher^{6#e}, Anna Lipzen³, Ryan Tillman¹, Eugene V. Shakirov^{7#f}, Xiaoyu Weng⁷, Ivone Torres-Jerez⁸, Brock Weers⁹, Daniel Conde¹⁰, Marilia R. Pappas¹¹, Lifeng Liu³, Andrew Muchlinski^{12#g}, Hui Jiang¹³, Christine Shyu^{13#h}, Pu Huang^{13#i}, Jose Sebastian^{13#j}, Carol Laiben^{13#k}, Alyssa Medlin^{13#l}, Sankalpi Carey^{13#m}, Alyssa A. Carrell¹⁴, Mariano Perales^{10,15}, Kankshita Swaminathan¹, Isabel Allona^{10,15}, Dario Grattapaglia¹¹, Elizabeth A. Cooper^{16#n}, Dorothea Tholl¹², John P. Vogel³, David J Weston¹⁴, Xiaohan Yang⁵, Thomas P. Brutnell¹⁷, Elizabeth A. Kellogg¹³, Ivan Baxter¹³, Michael Udvardi^{8#o}, Yuhong Tang⁸, Todd C. Mockler¹³, Thomas E. Juenger⁷, John Mullet⁹, Stefan A. Rensing^{4#p}, Gerald A. Tuskan⁵, Sabeeha S. Merchant^{6#e#q}, Gary Stacey², Jeremy Schmutz^{1,3*}

¹ HudsonAlpha Institute for Biotechnology, Huntsville, AL, USA

² Divisions of Plant Science and Biochemistry, National Center for Soybean Biotechnology, University of Missouri, Columbia, MO, USA

³ Joint Genome Institute, Lawrence Berkeley National Laboratory, Berkeley, CA, USA

⁴ Plant Cell Biology, Faculty of Biology, University of Marburg, Karl-von-Frisch-Str, Marburg, Germany

⁵ Center for Bioenergy Innovation, Oak Ridge National Laboratory, Oak Ridge, TN, USA

⁶ Department of Chemistry and Biochemistry and Institute for Genomics and Proteomics, University of California, Los Angeles, CA, USA

⁷ Department of Integrative Biology, University of Texas at Austin, Austin, TX, USA

⁸ Noble Research Institute, Ardmore, OK, USA

⁹ Department of Biochemistry and Biophysics, Texas A&M University, College Station, TX, USA

¹⁰ Centro de Biotecnología y Genómica de Plantas, Universidad Politécnica de Madrid, Instituto Nacional de Investigación y Tecnología Agraria y Alimentaria (INIA-CSIC), Madrid, Spain

¹¹ Laboratório de Genética Vegetal, EMBRAPA Recursos Genéticos e Biotecnologia, EPQB Final W5 Norte, Brasília, Brazil

¹² Department of Biological Sciences, Virginia Tech, Blacksburg, VA, USA

¹³ Donald Danforth Plant Science Center, St. Louis, MO, USA

¹⁴ Biosciences Division, Oak Ridge National Laboratory, Oak Ridge, TN, USA

¹⁵ Departamento de Biotecnología-Biología Vegetal, Escuela Técnica Superior de Ingeniería Agronómica, Alimentaria y de Biosistemas, Universidad Politécnica de Madrid, Madrid, Spain

¹⁶ Advanced Plant Technology Program, Clemson University, Clemson, SC, USA

¹⁷ Gateway Biotechnology Inc, St. Louis, MO, USA

*Corresponding authors, email: asreedasyam@hudsonalpha.org, jschmutz@hudsonalpha.org

^{#a} Current address: Texas A&M AgriLife Research and Department of Soil and Crop Sciences, Texas A&M University, College Station, TX, USA

^{#b} Current address: Department of Algal Development and Evolution, Max Planck Institute for Biology Tübingen, Tübingen, Germany

^{#c} Current address: GSK Vaccines GmbH, Emil-von-Behring-Str, Marburg, Germany

^{#d} Current address: Université Paris-Saclay, INRAE, AgroParisTech, Institut Jean-Pierre Bourgin (IJPB) Versailles, France

^{#e} Current address: Department of Plant and Microbial Biology and Department of Molecular and Cell Biology, QB3, University of California, Berkeley, Berkeley, CA, USA

^{#f} Current address: Department of Biological Sciences, Marshall University, Huntington, WV, USA

^{#g} Current address: Firmenich, San Diego, CA, USA

^{#h} Current address: Bayer Crop Science, St. Louis, MO, USA

^{#i} Current address: BASF Corporation, Durham, NC, USA

^{#j} Current address: Department of Biological Sciences, Indian Institute of Science Education and Research, Berhampur (IISER BPR), Odisha, India

^{#k} Current address: Propper Asset Management, 17 Research Park Drive, St. Charles, MO, USA

^{#l} Current address: Saginaw High School, 800 N Blue Mound Rd, Saginaw, TX, USA

^{#m} Current address: Invitae Corporation, 1400 16th Street, San Francisco, CA, USA

^{#n} Current address: Department of Bioinformatics and Genomics, University of North Carolina at Charlotte, Charlotte, NC, USA

^{#o} Current address: Center for Crop Science, The University of Queensland, St. Lucia, Brisbane, Australia

^{#p} Current address: Faculty of Chemistry and Pharmacy, University of Freiburg, Freiburg, Germany

^{#q} Environmental Genomics and Systems Biology, Lawrence Berkeley National Laboratory, Berkeley, CA, USA

65 ABSTRACT

66 Gene functional descriptions, which are typically derived from sequence similarity to experimentally validated
67 genes in a handful of model species, offer a crucial line of evidence when searching for candidate genes that
68 underlie trait variation. Plant responses to environmental cues, including gene expression regulatory variation,
69 represent important resources for understanding gene function and crucial targets for plant improvement
70 through gene editing and other biotechnologies. However, even after years of effort and numerous large-scale
71 functional characterization studies, biological roles of large proportions of protein coding genes across the plant
72 phylogeny are poorly annotated. Here we describe the Joint Genome Institute (JGI) Plant Gene Atlas, a public
73 and updateable data resource consisting of transcript abundance assays from 2,090 samples derived from 604
74 tissues or conditions across 18 diverse species. We integrated across these diverse conditions and genotypes
75 by analyzing expression profiles, building gene clusters that exhibited tissue/condition specific expression, and
76 testing for transcriptional modulation in response to environmental queues. For example, we discovered
77 extensive phylogenetically constrained and condition-specific expression profiles across many gene families
78 and genes without any functional annotation. Such conserved expression patterns and other tightly co-
79 expressed gene clusters let us assign expression derived functional descriptions to 64,620 genes with
80 otherwise unknown functions. The ever-expanding Gene Atlas resource is available at JGI Plant Gene Atlas
81 (<https://plantgeneatlas.jgi.doe.gov>) and Phytozome (<https://phytozome-next.jgi.doe.gov>), providing bulk access
82 to data and user-specified queries of gene sets. Combined, these web interfaces let users access differentially
83 expressed genes, track orthologs across the Gene Atlas plants, graphically represent co-expressed genes, and
84 visualize gene ontology and pathway enrichments.

85

86 INTRODUCTION

87 The flowering plant, *Arabidopsis thaliana*, has served as a model for functional genomics over the past two
88 decades. While the goal of functionally characterizing each *A. thaliana* gene by the year 2010 (Koornneef and
89 Meinke 2010) has yet to be fully realized, many large-scale studies, such as gene knock-out collections for
90 reverse genetics, have tested the phenotypic effects nearly half of *A. thaliana* protein-coding genes (Berardini et
91 al. 2015). These experimentally validated loci, and a massive set of predicted and curated gene functions form
92 the foundation for gene characterization across 400M years of plant evolution.

93 Despite the potential for homology-based functional annotations across plants, putative gene functions in non-
94 model plants are sparse, often containing a majority of genes with no functional descriptions. These knowledge
95 gaps are undoubtedly due to the phylogenetic and functional scale of plant diversity. At one extreme, DNA or
96 protein sequences may have diverged so that no genes have obvious *A. thaliana* homologs. However, even with
97 homology, assigning gene function to distantly related plants assumes function is evolutionarily conserved. This
98 assumption is clearly violated in many situations: flowering plants have evolved diverse adaptive traits,
99 specialized organs/tissues, and environmental responses, all of which are poorly captured by a single model
100 organism. Further, gene neofunctionalization, subfunctionalization and gene cooption may invalidate direct
101 superimposition of gene annotation from one species to another (C. Li et al. 2012; Nicotra et al. 2010; Raissig et
102 al. 2017). The addition of other model species, including *Brachypodium distachyon*, *Oryza sativa*, and
103 *Physcomitrium patens*, has helped fill gaps in homology-based functional annotations. However, 16.1-56.9% (M
104 $= 27.8$; $SD = 10.06$) of protein coding genes across the plant phylogeny remain poorly characterized
105 (**Supplemental Fig. 1**) (Gollery et al. 2006, 2007; Rhee and Mutwil 2014).

106 Incomplete gene functional annotations are not only due to an overreliance on few genetic model organisms,
107 but also an inability to link experimental evidence across species. However, centralized functional databases
108 containing information generated from new experiments such as ongoing large-scale transcriptome projects
109 and genome-wide association studies could accelerate gene function discovery. Even with a central repository,
110 interpretation and integration across diverse studies is difficult because experimental and analytical protocols
111 are rarely standardized. For example, different sample collection, RNA isolation, library construction protocols,
112 and sequencing platforms can result in significant variation in sequence coverage and estimates of gene
113 expression (Levin et al. 2010; Ross et al. 2013; Sudmant, Alexis, and Burge 2015; Yu et al. 2014). This among-
114 experiment variation reduces the accuracy and precision of comparisons across species and studies, which
115 directly limits putative gene function inference from transcript abundance profiles.

116 Here, we present an updateable large-scale dataset and a suite of experimental protocols to facilitate functional
117 gene prediction across the diversity of plants. Crucially, we have developed experimental conditions, tissue
118 types, and analytical protocols that permit comprehensive analysis of gene expression across plants. We
119 applied these conditions and collected 2,090 tissue samples from 18 plant species spanning single-celled

120 algae, bryophytes, and flowering plants. This integrated dataset (1) forms a foundation to improve gene
121 functional annotations, (2) facilitates cross-species comparative transcriptomics within controlled environmental
122 and laboratory conditions, and (3) permits high-powered tests of gene regulatory evolution across
123 phylogenetically diverse plant genomes. To demonstrate this functionality, we cataloged the expression profiles
124 of annotated genes, and built co-expressed clusters of genes that exhibited tissue/condition specific
125 expression patterns including responses to changes in nitrogen (N) regimes, abiotic stressors, and
126 developmental stages. We systematically assigned expression derived functional descriptions to an average of
127 40.6% ($SD = 12.6$) of annotated genes in the assessed genomes, 9.5% of which previously had no known
128 function. This substantial transcriptomic resource is available to the research community at JGI Plant Gene
129 Atlas (<https://plantgeneatlas.jgi.doe.gov>) and through Phytozome, the JGI Plant Portal, at [https://phytozome-](https://phytozome-next.jgi.doe.gov)
130 [next.jgi.doe.gov](https://phytozome-next.jgi.doe.gov) (Goodstein et al. 2012).

131

132 SCOPE OF DATA GENERATED

133 We developed the JGI Gene Atlas from 15.4 trillion sequenced RNA bases (Tb) and 2,090 RNA-seq samples
134 across 9 JGI plant flagship genomes and 9 other reference plants (**Table 1**). For each of the sequenced plants,
135 we collected tissue samples representing appropriate developmental stages, growth conditions, tissues, and
136 abiotic stresses (**Fig. 1**). To reduce residual environmental variance, we followed standard growth conditions
137 including light quality, quantity and duration, temperature, water, growth media, and nutrients. Experimental
138 treatments were applied using standardized methods across all species (see Methods).

139

140 **Table 1 | JGI Plant Gene Atlas species.** Genome annotation versions of 18 diverse plants included in the current release.

141

Genome	Version	Project	Taxonomy ID	Source
<i>Arabidopsis thaliana</i>	TAIR10	Gene Atlas	3702	phytozome-next.jgi.doe.gov/info/ATHaliana_TAIR10
<i>Brachypodium distachyon</i>	v3.1	Gene Atlas	5143	phytozome-next.jgi.doe.gov/info/Bdistachyon_v3_1
<i>Chlamydomonas reinhardtii</i>	v5.6	Gene Atlas	3055	phytozome-next.jgi.doe.gov/info/Creinhardtii_v5_6
<i>Eucalyptus grandis</i>	v2.0	Gene Atlas	71139	phytozome-next.jgi.doe.gov/info/Egrandis_v2_0
<i>Glycine max</i>	Wm82.a4.v1	Gene Atlas	3847	phytozome-next.jgi.doe.gov/info/Gmax_Wm82_a4_v1
<i>Kalanchoë fedtschenkoi</i>	v1.1	Gene Atlas	63787	phytozome-next.jgi.doe.gov/info/Kfedtschenkoi_v1_1
<i>Lupinus albus</i>	v1.1	Non-JGI	3870	phytozome-next.jgi.doe.gov/info/Lalbus_v1
<i>Medicago truncatula</i>	Mt4.0v1	Gene Atlas	3880	phytozome-next.jgi.doe.gov/info/Mtruncatula_Mt4_0v1
<i>Panicum hallii</i> var. <i>filipes</i>	v3.1	Gene Atlas	907226	phytozome-next.jgi.doe.gov/info/Phallii_v3_1
<i>Panicum hallii</i> var. <i>hallii</i>	v2.1	Gene Atlas	1504633	phytozome-next.jgi.doe.gov/info/PhalliiHAL_v2_1
<i>Physcomitrium patens</i>	v3.3	Gene Atlas	3218	phytozome-next.jgi.doe.gov/info/Ppatens_v3_3
<i>Populus trichocarpa</i>	v4.1	Gene Atlas	3694	phytozome-next.jgi.doe.gov/info/Ptrichocarpa_v4_1
<i>Panicum virgatum</i>	v5.1	Gene Atlas	38727	phytozome-next.jgi.doe.gov/info/Pvirgatum_v5_1
<i>Sorghum bicolor</i>	v3.1.1	Gene Atlas	4558	phytozome-next.jgi.doe.gov/info/Sbicolor_v3_1_1
<i>Sorghum bicolor</i> var <i>Rio</i>	v2.1	JGI-CSP	4558	phytozome-next.jgi.doe.gov/info/SbicolorRio_v2_1
<i>Sphagnum angustifolium</i>	v1.1	Gene Atlas	53036	phytozome-next.jgi.doe.gov/info/Sfallax_v1_1
<i>Setaria italica</i>	v2.2	Gene Atlas	4555	phytozome-next.jgi.doe.gov/info/Sitalica_v2_2
<i>Setaria viridis</i>	v2.1	Gene Atlas	4556	phytozome-next.jgi.doe.gov/info/Sviridis_v2_1

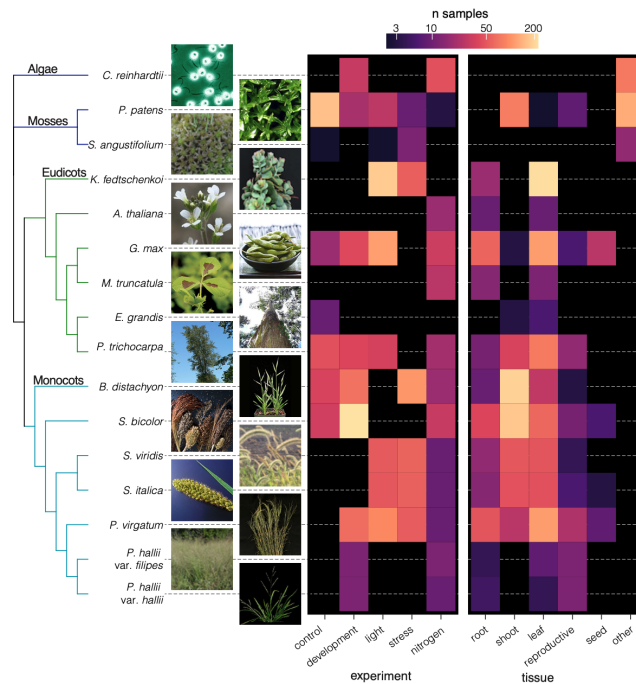
142

Sreedasyam et al. 2022 (preprint) JGI Plant Gene Atlas

143 We sought to limit among-experiment measurement and environmental variation by using identical molecular
144 methods to extract (RNA integrity number, RIN ≥ 5 and at least 1 μg of total RNA) and sequence (Illumina
145 stranded, paired-end 2x150 RNA-seq libraries) high-quality RNA. All samples were quality tested and
146 sequenced at JGI. The resulting transcript abundance assays were highly correlated across biological replicates
147 within conditions, tissues, and genotypes (**Supplemental Data 1**), which provides evidence that our gene
148 expression measurements are highly accurate and robust.

149 We also demonstrated that the JGI Gene Atlas is updateable, with a new reference genome version and even
150 with sequence data derived from other experiments and sequencing facilities. To accomplish this, we included
151 *S. bicolor* 'Rio' (sweet sorghum, $n_{\text{samples}} = 94$) (Cooper et al. 2019) from JGI's Community Science Program
152 project and *Lupinus albus* (white lupin) cluster root tissue ($n_{\text{samples}} = 72$) (Hufnagel et al. 2020) from a non-JGI
153 project. A comprehensive list of all samples available so far is in **Supplemental Data 2** and
154 <https://plantgeneatlas.jgi.doe.gov>. Our custom pipeline to analyze expression levels of protein-coding genes is
155 outlined in **Supplemental Fig. 2**.

156



157

158

159 **Figure 1 | The phylogenetic context and scope of Gene Atlas RNA-seq samples.** The 16 genomes are ordered by their
160 phylogenetic position, visualized on the left as a cladogram without branch lengths that was constructed from 10 single-copy
161 orthologs. Tips are labeled with genome names and thumbnail photos. Photo credit given on Phytozome.

162

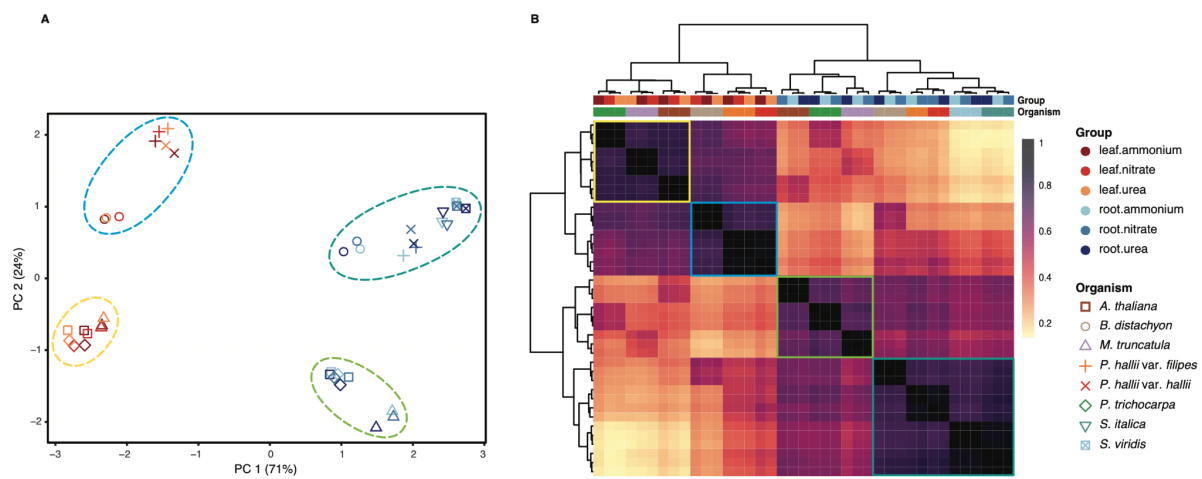
163 OVERVIEW OF THE TRANSCRIPTOMIC LANDSCAPE OF GENE ATLAS PLANTS

164 **Developing a baseline of evolutionarily conserved gene expression.** Across all 18 species, 47-87% (mean =
165 73%) of annotated genes were transcriptionally active (FPKM > 1). To test for conserved and divergent
166 expression levels across the 18 species, we applied the traditional method of comparing single-copy orthologs
167 across species. While powerful, restricting tests to orthologs based on gene sequences can be problematic
168 across evolutionarily diverged lineages. For example, given the phylogenetic distance and nested whole-
169 genome duplications among our sampled species, we were only able to find 2,066 one-to-one orthologous
170 protein-coding genes (**Supplemental Data 3**) across just eight of the vascular plant genomes. Furthermore,
171 such single-copy orthologs have evolutionarily conserved sequences and likely gene functions, permitting
172 better homology-based functional descriptions (89.01% with good functional descriptions) than genome-wide
173 averages (83.8%, Fisher's exact test odds = 1.607, $P = 5.495\text{e-}12$). Nonetheless, we observed 227 (10.98%)
174 genes with 1:1 orthologs and consistent expression among species, but weak functional descriptions
175 (**Supplemental Data 4**). Given the expected paucity of multi-genome single-copy orthologs, we also addressed
176 the challenge of finding genes with similar expression across species by analyzing pairwise single-copy

177 orthologs to a single reference genome, *A. thaliana*. Overall, we identified 6,018 unique *Arabidopsis* orthologs
178 that showed conserved expression patterns across multiple species. Surprisingly, these genes include 660
179 (11%) with little to no known functional description, making these genes rational targets for functional
180 characterization studies (**Supplemental Data 5**). Identifying and improving the functional characterizations of
181 such genes was one of the objectives of the Gene Atlas experiment. Genes with single-copy orthologs in *A.*
182 *thaliana* and consistent expression were significantly enriched in transcription factors ($n = 501$, 8.3%; Fisher's
183 exact test odds ratio = 1.507, $P = 4.26e-13$), suggesting that potential regulators of different biological
184 processes are strongly conserved across the plant species (Keightley and Hill 1990). These observed
185 evolutionarily conserved expression patterns inform functional details that complement direct sequence data
186 comparisons.

187 In contrast to these ortholog-constrained analyses, co-expression analyses are agnostic to orthology, which
188 dramatically increases the number of genes that can be analyzed, providing a broader perspective on gene
189 expression regulatory evolution. For example, multidimensional scaling and hierarchical clustering revealed that
190 phylogenetically neighboring species have more similar expression profiles across tissues and nitrogen
191 treatments than more distantly related species (Mantel $R > 0.63$, $P < 0.04$) (**Fig. 2**). However, the phylogenetic
192 signal of co-expression was dwarfed by variation among tissues, where far more of the total co-expression
193 clustering across nitrogen source treatments was driven by patterns among tissues than genetic distance
194 among species (tissues correlated with the first canonical correspondence analysis axis, which explains 41.46%
195 of the variation), suggesting that genes in closely related species exhibit similar transcriptional profiles across
196 tissues and conditions likely owing to the accumulation of evolutionarily conserved regulatory elements.

197



198

199

200 **Figure 2 | Global patterns of gene expression across eight vascular plants.** Multidimensional scaling based on the
201 expression of 2,066 single-copy orthologous genes in two tissues and three nitrogen treatment conditions show predominant
202 clustering first by tissues and then by clade (mono-, dicots) (A). Hierarchical clustering based on Pearson correlation coefficients of
203 \log_2 transformed normalized expression data (B).

204

205 **Patterns of tissue-specific gene expression across 18 species and >400M years of plant evolution.**

206 Tissue-specific expression complements global co-expression analyses by defining potential gene function
207 associated with an organ or tissue. The major drawback of this approach results from morphological
208 differences among species. For example, in *Chlamydomonas*, a single-celled organism, transcriptionally active
209 genes in a given condition represent expressed genes in the organism as a whole, whereas multicellular
210 organisms exhibit gene expression variation across different cell subtypes. Furthermore, the mosses sampled
211 here lack root systems, flowers, seeds or easily sampled reproductive organs. Even the far more closely related
212 flowering plants have functionally divergent homologous structures, such as root nodules, panicles, florets,
213 sepals, and rhizomes. As such, analysis of tissue-specific expression must be somewhat phylogenetically
214 constrained and condensed into large-scale functional tissue types (**Fig. 1**).

215 Our data suggest that large proportions of annotated genes (27-68%, $M = 44.7$; $SD = 12.7$) are commonly
216 expressed (FPKM > 1) in multiple tissues (**Supplemental Data 6**), confirming that many genes serve multiple
217 functions across tissues and environments. However, there was considerable among-tissue variation across

218 species (ANOVA $F = 70.01$, $df = 16$, $P < 2e-16$) where gene expression is driven by variation among tissues or
219 conditions (**Supplemental Data 6**). Such variably expressed genes may have evolved diverse functions
220 depending on the regulatory environment across cell types.

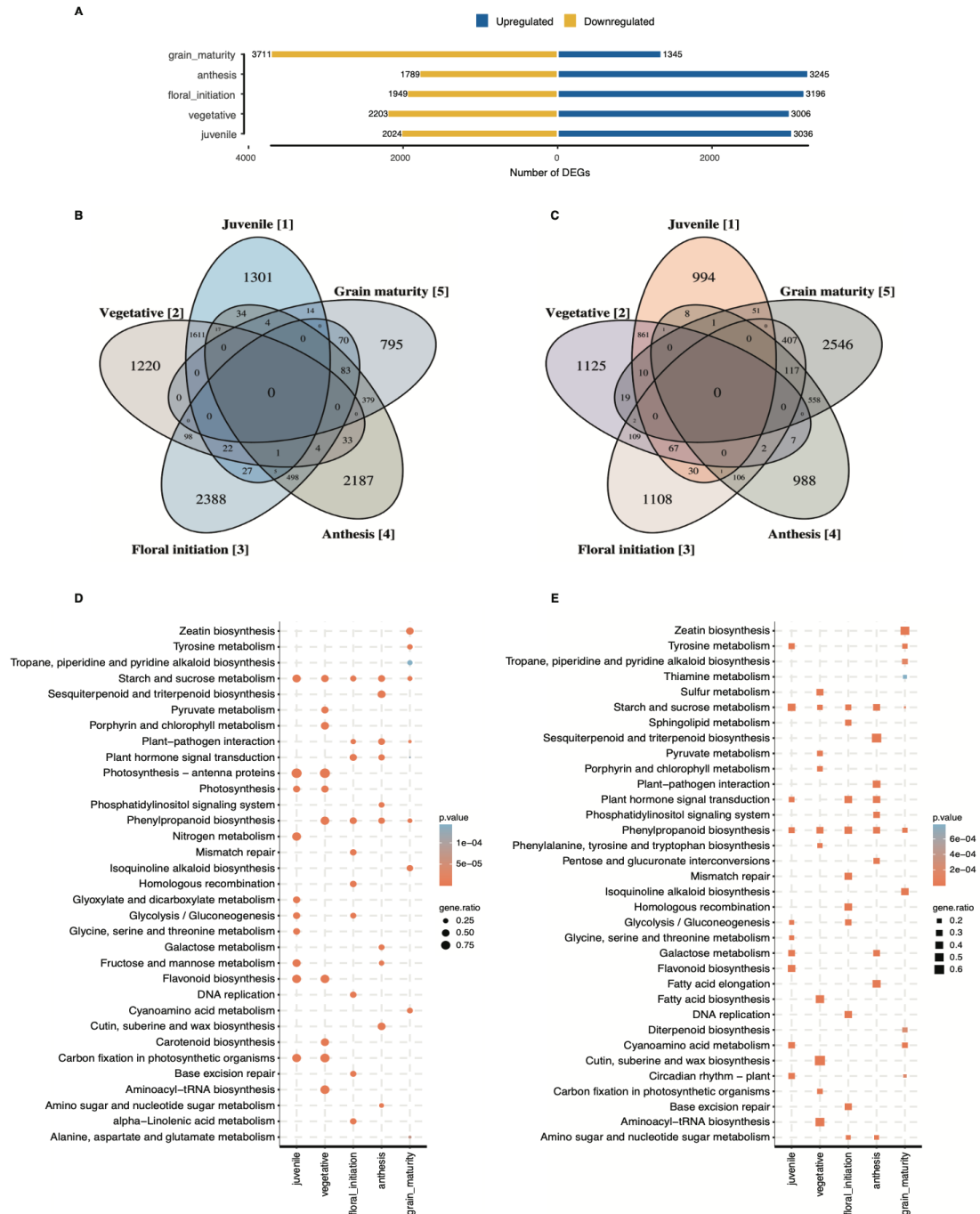
221 Despite considerable across-tissue expression, we observed 220,218 (32.1%) of all genes with high expression
222 specificity to a single tissue or condition. To identify genes exhibiting such strong tissue or condition specific
223 expression, we used the Tau method (Yanai et al. 2005) which accounts for the number of unique sample types
224 and produces consistently robust results with highest correlation between datasets of varying sizes
225 (Kryuchkova-Mostacci and Robinson-Rechavi 2017). Using this method, we identified genes specific to (1)
226 reproductive and root tissue in *S. italica*, (2) leaf, inflorescence, and whole floret in switchgrass, (3) leaf, leaf
227 blade, dry seed, and imbibed seed in *S. bicolor*, and (4) stem and flower related gene sets in *Brachypodium*. Of
228 all the standard plant tissues, stem and leaf had the fewest uniquely expressed genes (two-tailed unpaired
229 Welch's t-test, $P = 8.338e-06$) while roots followed by flower tissues were most unique (two-tailed unpaired
230 Welch's t-test, $P = 2.547e-10$). Groups of genes with greater expression proclivity towards spores, protonema
231 and leaflet were recognized in *Physcomitrium*; drought and high temperature in *Sphagnum*; and towards seed,
232 root tip, lateral root, and nodules in soybean (**Supplemental Data 7, 8**). These gene sets were largely
233 overrepresented in GO biological processes known for each tissue or condition (**Supplemental Data 9**). Genes
234 and their promoter regions with such marked expression specificity represent valuable tissue-specific reporters
235 and targets for plant genetic engineering applications.

236

237 **Transcription modulation across developmental stages.** Developmental time-courses represent a
238 particularly powerful experiment to understand gene function and the dynamics of transcript abundance. As an
239 example of such a time course, we evaluated the regulation of gene expression in leaf tissue in five
240 developmental stages of *Sorghum bicolor* (juvenile, vegetative, floral initiation, anthesis and grain maturity).
241 Overall, we identified 13,992 unique DEGs (n total annotated genes= 34,211) across the five developmental
242 stages (**Fig. 3A, 3B, 3C**). KEGG pathway enrichments of up-regulated differentially expressed genes were
243 largely consistent with physiological expectations: photosynthesis, carbohydrate and N metabolism terms were
244 overrepresented in juvenile/vegetative stages ($P < 0.05$, hypergeometric test), floral initiation/anthesis stages
245 were enriched in reproductive organ development and hormone signal transduction, and grain maturity stage
246 were enriched for amino acid metabolism and transport, and zeatin and tyrosine metabolism (**Fig. 3D, 3E**). We
247 observed the enrichment pattern to be reversed among downregulated genes in different stages, e.g., plant-
248 pathogen interaction and plant hormone signal transduction were suppressed in juvenile and vegetative stages
249 whereas photosynthesis, carbohydrate and N metabolism related pathways were among those suppressed in
250 late developmental stages (**Supplemental Fig. 3**). These overrepresented pathways among DEGs at each stage
251 illustrate the key biological events over the growing season, e.g., as juveniles the *S. bicolor* are collecting
252 energy to increase the biomass, and as they flower and mature, they express defense mechanisms, and finally,
253 with grain maturity, they reduce photosynthesis and slow down nutrient acquisition. The *S. bicolor* dataset
254 provides an example of high-resolution characterization of gene expression changes and insight into the
255 molecular responses of the plant across developmental stages represented by the Gene Atlas dataset.

256

Sreedasyam et al. 2022 (preprint) JGI Plant Gene Atlas



257

258

259

260

261

262

263

264

265

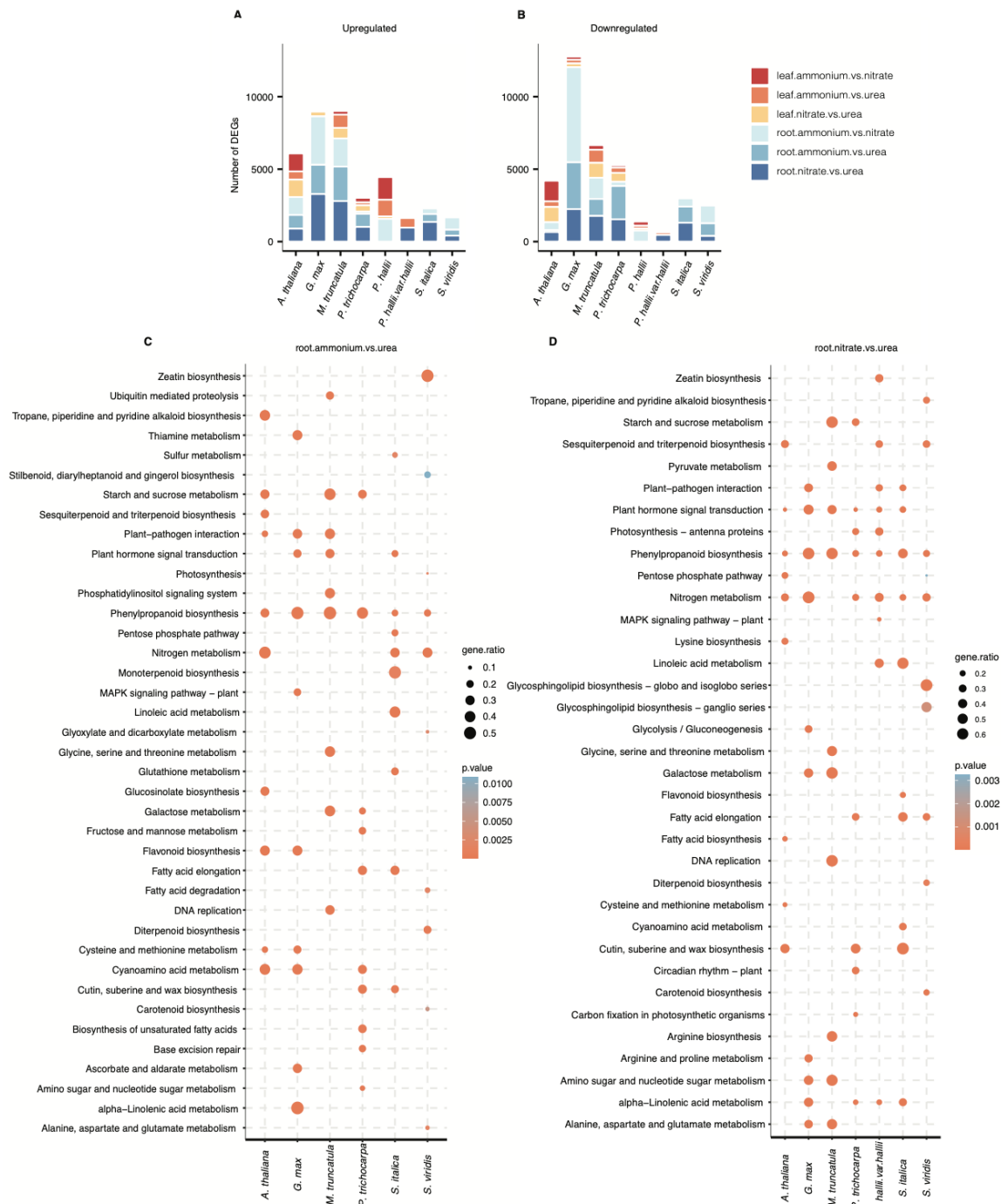
266

267

268

Figure 3 | Differentially expressed gene comparison across five developmental stages in *Sorghum bicolor*. Numbers of differentially expressed genes across developmental stages (A). Venn diagrams of up-regulated (B) and down-regulated genes that are unique and shared between developmental stages (C). Top 10 KEGG metabolic pathway enrichments ($P < .05$, hypergeometric test) of up-regulated differentially expressed genes in each of the five developmental stages (D) and up-regulated genes unique to each stage (E). 'gene_ratio' represents the ratio of number of DEGs over the number of genes annotated specific to the pathway.

269 **Transcriptional responses to different N sources.** Tissue-specific gene expression regulatory responses to
270 environmental cues are often evolutionarily conserved. These conserved responses offer a framework to test
271 hypotheses about gene function as it relates to environmental sensitivity. A particularly powerful experiment
272 adjusts the amount and type of necessary resource available. Drought, light and nutrient availability
273 manipulations have provided strong evidence for gene function across the diversity of plants (Faye et al. 2022);
274 (Zhang et al. 2021); (Huang, Zhao, and Chory 2019); (Swift et al. 2020); (Y. Li et al. 2022). In addition to providing
275 evidence for the function of specific candidate genes' responses to environmental stimuli, highly controlled
276 manipulations, like our nitrogen source experiments, offer a framework to compare the relative roles of gene
277 families and molecular pathways.
278 To understand gene expression underpinnings of N metabolism, we contrasted transcript abundance in
279 aboveground and root tissues of each Gene Atlas species (where available, see **Fig. 1**) grown on N from three
280 sources: urea, ammonium (NH_4^+), and nitrate (NO_3^-) (**Supplemental Data 10**). Since our experiments had similar
281 statistical power and biological replicates among species and conditions, the total number of DEGs is a strong
282 indicator of the transcriptional effects of different N sources. The most striking patterns were those related to
283 tissue-specific gene expression variation within genotypes (**Fig. 4A, 4B**). For example, the root transcriptome
284 was more responsive than aboveground tissues in all eudicot genotypes (Mann-Whitney U-test, $P = 5e-04$)
285 except *Arabidopsis* (two-tailed unpaired Welch's t-test, $P = 0.4526$). We observed consistent enrichments of N
286 metabolism pathway genes among differentially expressed genes between treatments across many species,
287 which demonstrates that this experiment elicits molecular responses of genes with homologs in genetic model
288 species.
289 Despite the power of discovering enriched groups of genes with similar and expected functional annotations, a
290 major goal of the Gene Atlas is to provide a framework to discover novel gene functions and interactions. As
291 such, we were excited to find starch and sucrose metabolism, and phenylpropanoid biosynthesis pathways
292 overrepresented in upregulated DEGs. Indeed, many of the DEGs we identified in pairwise comparisons
293 between N-sources are not directly involved in N metabolism. For example, genes associated with plant-
294 pathogen interaction, plant hormone signal transduction, and carbohydrate metabolism were abundant (**Fig.**
295 **4C, 4D, Supplemental Fig. 4**). Similar observations were reported previously in *Sorghum* genotypes with
296 varying N-stress tolerance subjected to N-limiting conditions (Gelli et al. 2014). Notably, nitrogen and amino
297 acid metabolism-related pathways were overrepresented mainly in DEGs in nitrate vs. urea comparison. Such
298 comparisons highlight differences in plant's response to NO_3^- as a sole N source compared to NH_4^+ at the
299 metabolic level.



300

301 **Figure 4 | Transcriptional response of Gene Atlas plants towards NH_4^+ and NO_3^- compared to urea as the sole nitrogen**
 302 **source in root and leaf tissues.** Numbers of genes differentially upregulated (A) and numbers of genes differentially
 303 downregulated in response to changing nitrogen regime (B). Top 10 KEGG metabolic pathway enrichments ($P < .05$,
 304 hypergeometric test) in up-regulated differentially expressed genes in roots from Gene Atlas plants in ammonia vs. urea (C)
 305 and nitrate vs. urea treatment comparisons (D). 'gene.ratio' represents the ratio of number of DEGs over the number of genes
 306 annotated specific to the pathway.

307

308

309

310

INFERRING GENE FUNCTION FROM PATTERNS OF GENE EXPRESSION

311

312

313

314

315

316

317

318

319

320

321

322

323

324

325

326

327

328

329

330

331

332

333

334

335

336

337

338

339

340

341

342

343

344

345

346

347

348

349

350

351

352

353

354

355

356

357

358

359

360

361

362

363

364

365

366

Variation in co-expression network topologies. Genes with similar expression patterns across diverse environmental conditions and tissues tend to serve similar biological functions across distantly related species and can be detected by co-expression clustering algorithms. For example, clusters of genes associated with a specific tissue or condition may be crucial for plant development or response to environmental cues. These strongly conserved tissue- and treatment-specific expression patterns facilitate biological gene function extrapolating from expression studies in one organism to close phylogenetic neighbors. To identify modules with such coherent expression patterns, we constructed 30 weighted gene co-expression networks (Langfelder and Horvath 2008) and 148 highly significant (min KME = 0.7, cut height = 0.25) co-expression modules within species and across different sets of tissues and conditions. Of these, 21 modules were significantly correlated with stress treatments (i.e., heat, cold, drought, salt, and wound stresses), 10 with N treatments, and 33 with other experimental conditions (**Supplemental Data 11**). Tissue-specific modules were also very common, e.g., root tissue-specific modules ($n = 11$), contained genes with GO terms enriched in responses to stimulus, oxidation-reduction process (Manzano et al. 2014; Passaia et al. 2014) and hydrogen peroxide metabolism (Ma et al. 2014) that are relevant to root functions (Bruex et al. 2012; Kogawara et al. 2014; W. Li, Lan, and 3.948 2015; Loreti et al. 2005). Leaf specific modules ($n = 11$) were enriched for phototropism, thylakoid membrane organization, pigment biosynthetic process, phototropism, and carbon fixation (**Supplemental Data 12**), suggesting that genes within the same module are associated with the same or interconnected biological functions.

Inferring transcription factor functions from co-expressed genes. Genes showing highest connectivity with neighboring genes within a module, referred to as hub genes, are likely involved in preserving multi-gene regulatory variation and thus network integrity, potentially as trans-regulatory elements like transcription factors. We determined the top 10 most highly connected hub genes within each module. Across all the co-expression networks 87 hub genes belonged to transcription factor (TF) families (via PlantTFDB; (Jin et al. 2017)) (**Supplemental Data 13**), a slight but not significant enrichment of TFs relative to the genomic background (% hub TFs = 6.21%, background TFs = 5.23%, Fisher's exact test odds ratio = 0.834, $P = 0.104$). TFs with many connections are presumed to be most influential in regulating the expression of modular genes in co-expression networks (Mukhtar et al. 2011). Under this premise, we further explored the overrepresented TF families among the hub genes. Most represented TF families in N treatment modules were MYB, WRKY, and NAC. Similar observations were made by Canales *et al.* (Canales et al. 2014) from Arabidopsis root transcriptomic data generated under contrasting N conditions. As shown in previous studies (Ghazalpour et al. 2006; Horvath et al. 2006; Liu, He, and Deng 2021; Miller, Oldham, and Geschwind 2008; Torkamani et al. 2010; Voineagu et al. 2011), hub genes play key roles in orchestrating module behavior and provide a specific focus for investigations into trait or condition related modules.

Expression derived function descriptions (EDFD). To evaluate how well the predicted gene function descriptions of Gene Atlas plants illustrate validated gene functions, we categorized currently assigned functional descriptions available at Phytozome as genes with good (GGF) and poor (GPF) function descriptions using an augmented dictionary lookup approach that incorporates weighting for negative, positive, and adversative keywords. Overall, 16% to 56% of the functional descriptions are GPF across the plants, with a large percentage of such genes not having a known function (**Supplemental Fig. 1**) (Gollery et al. 2006; Rhee and Mutwil 2014). We then assigned EDFD to the two subsets using results from tissue and condition specific expression groups, DEGs unique to a single contrast and co-expression network analysis along with ortholog function descriptions derived from nearest phylogenetic neighbors (see Methods).

Using this method, we added additional biological information to an average of 40.6% ($SD = 12.6$) of genes (excluding orthology based function descriptions) in these plant genomes (**Table 2; Supplemental Data 14**). For example, in the case of *S. bicolor*, 5,357 (15.65% of the total) genes lacked sequence homology-based function descriptions, 24,406 had good functional descriptions while overall 9,723 had poor descriptions. Gene Atlas expression-based functional descriptions were assigned to a total of 20,259 genes, of which 14,891 (43.63% of total annotated genes) had good functional descriptions and 5,368 (15.73%) had poor descriptions. To verify the reliability of the assigned functional associations, GO enrichment analysis of genes assigned with descriptions based on leaf and root samples was performed. We observed significant enrichment for photosynthesis, chloroplast organization, chlorophyll biosynthetic process and plastid translation ($P < .05$, Fisher's exact test) in leaf related EDFDs; and cell wall loosening (Somssich, Khan, and Persson 2016), water transport and xyloglucan biosynthetic process (Peña et al. 2012) ($P < .05$, Fisher's exact test) in root related

EDFDs. Similar analysis in *Brachypodium* genes with assigned descriptions based on abiotic stress experiments (i.e., cold, heat, drought, and salt stress) showed significant enrichment for regulation of cellular response to alkaline pH, response to cold, heat, and positive regulation of response to oxidative stress ($P < .05$, Fisher's exact test). Likewise, among genes annotated based on flower samples, specification of floral organ identity, fruit wall development and sporopollenin biosynthetic process were among the top enriched GO terms ($P < .05$, Fisher's exact test). These results indicate that the assigned functional descriptions show strong biological role predictability and the approach here aids in expanding our current understanding of plant gene functions.

375

Table 2 | Summary of assigned expression derived function descriptions (EDFD) to Gene Atlas. Number of annotated genes and the percentage of genes with good function descriptions (GGF), poor function descriptions (GPF) categorized using an augmented dictionary lookup approach that incorporates weighting for negative, positive, and adversative keywords and percentage of genes assigned with expression derived function descriptions.

Genome	n.genes	% GGF	% assigned (GGF)	% GPF	% assigned (GPF)	n.assigned	% assigned (total)
<i>A. thaliana</i>	27,416	83.86	32.43	16.14	5.573	10,418	38.00
<i>B. distachyon</i>	34,310	72.56	34.17	27.44	13.19	16,247	47.35
<i>C. reinhardtii</i>	17,741	43.08	12.6	56.92	15.98	5,070	28.58
<i>E. grandis</i>	36,349	79.74	28.63	20.26	3.997	11,858	32.62
<i>G. max</i>	52,872	80.37	47.25	19.63	11.33	30,971	58.58
<i>K. fedtschenkoi</i>	30,964	82.01	39.56	17.99	7.644	14,615	47.20
<i>M. truncatula</i>	50,894	67.94	23.66	32.06	5.285	14,731	28.94
<i>P. hallii</i>	33,805	72.65	34.97	27.35	8.656	14,746	43.62
<i>P. hallii</i> HAL	33,263	73.36	31.16	26.64	7.946	13,007	39.10
<i>P. patens</i>	32,926	55.44	19.35	44.56	14.06	11,003	33.42
<i>P. trichocarpa</i>	34,699	82.31	39.57	17.69	7.997	16,507	47.57
<i>P. virgatum</i>	80,278	69.2	39.73	30.8	14.15	43,251	53.88
<i>S. bicolor</i>	34,129	71.51	43.63	28.49	15.73	20,259	59.36
<i>S. bicolor</i> Rio	35,490	69.16	15.04	30.84	4.765	7,029	19.81
<i>S. fallax</i>	25,100	78.31	32.36	21.69	9.183	10,427	41.54
<i>S. italica</i>	34,584	77	39.37	23	10.78	17,344	50.15
<i>S. viridis</i>	38,334	70.43	35.99	29.57	12.74	18,680	48.73
<i>L. albus</i>	38,258	78.17	11.01	21.83	2.415	5,138	13.43

380

To help investigators target important genes for additional functional studies, we ranked the biological relevance of genes using a scoring methodology based on expression patterns of genes identified using tissue/condition specificity, differential expression, co-expression, hub status in a co-expression module and consensus expression across species. Gene orthologs with similar expression profiles in two or more species were given additional scores derived from the phylogenetic distance, i.e., larger the divergence time higher the score (see Methods). We identified a total of 656 top ranked genes across Gene Atlas plants (604 have orthologs in ≥ 5 plants; 40 of which have orthologs in ≥ 10 of evaluated plants) that have poor functional information but with the potential to improve our understanding of plant biology and form a list of prioritized targets for future experimental investigations (**Table 3; Supplemental Data 15**).

390

391

392

393

394 **Table 3 | Prioritized top ranked genes with poor functional descriptions for future experimental investigations.** Genes
 395 were given scores based on expression patterns identified from i) unique differential expression in a single contrast, ii)
 396 tissue/condition specific expression and iii) biologically relevant co-expression modules (each given a score of 2) while hub
 397 genes in a co-expression module were given a score of 4. Gene orthologs with similar expression profiles were given
 398 additional scores derived from the phylogenetic distance. Total score was calculated as the aggregate of individual scores.
 399 Top ranked genes (two per species) are represented here.
 400

Organism	Gene ID	Score						Arabidopsis orthologs
		Differential expression	Condition specific expression	Co-expression	Hub gene	Consensus expression	Total	
<i>A. thaliana</i>	AT2G20080	2	2	2	0	21.91	27.91	AT2G20080
	AT4G28840	0	2	2	0	21.91	25.91	AT4G28840
<i>B. distachyon</i>	Bradi1g38210	0	2	2	0	10.7	14.7	AT2G42760
	Bradi2g23445	0	0	2	0	11.69	13.69	AT5G02090; AT2G37750
<i>C. reinhardtii</i>	Cre02.g078550	0	2	2	4	0	8	
	Cre02.g092700	0	2	2	4	0	8	
<i>E. grandis</i>	Eucgr.B00604	0	2	2	0	16.57	20.57	AT5G08050
	Eucgr.F01122	0	2	2	0	17.12	21.12	
<i>G. max</i>	Glyma.13G227500	0	0	2	0	20.28	44.56	AT1G33055
	Glyma.16G013600	0	0	2	0	20.84	45.68	AT3G14280
<i>K. fedtschenkoi</i>	Kaladp0065s0016	0	0	2	0	19.79	21.79	AT4G28840; AT2G20080
	Kaladp0965s0006	2	0	2	0	26.23	30.23	AT2G30230; AT1G06980
<i>M. truncatula</i>	Medtr2g079300	2	2	2	0	18.11	24.11	
	Medtr3g031140	0	2	2	0	27.28	31.28	AT2G30230; AT1G06980
<i>P. hallii var. filipes</i>	Pahal.3G090000	2	2	2	0	13.2	19.2	AT5G02160
	Pahal.7G305700	2	2	2	0	12.05	18.05	AT4G21445
<i>P. hallii var. hallii</i>	PhHAL.3G160400	0	0	2	0	14.55	16.55	
	PhHAL.5G229300	2	2	2	0	11.532	17.532	AT5G62770; AT3G27880; AT1G23710; AT1G70420
<i>P. patens</i>	Pp3c11_15500	2	2	2	4	0	10	
	Pp3c13_2427	0	2	2	4	0	8	
<i>P. trichocarpa</i>	Potri.018G084100	2	2	2	0	19.79	25.79	AT4G28840; AT2G20080
	Potri.003G193400	2	0	2	0	20.89	24.89	
<i>P. virgatum</i>	Pavir.5NG404000	0	0	2	0	13.64	15.64	
	Pavir.2NG640501	0	2	2	0	9.72	13.72	AT5G13720
<i>S. bicolor</i>	Sobic.009G229000	0	0	2	4	13.35	19.35	AT4G28840; AT2G20080
	Sobic.001G118400	2	2	2	0	10.44	16.44	AT1G73885
<i>S. bicolorRio</i>	SbRio.08G154700	0	2	2	0	12.31	16.31	AT5G08050
	SbRio.10G134000	0	2	2	0	12.05	16.05	AT4G01150
<i>S. angustifolium</i>	Sphfalx02G142200	2	2	2	4	0	10	
	Sphfalx11G077900	2	2	0	0	4.5	8.5	AT3G03341
<i>S. italica</i>	Seita.9G407600	2	0	2	0	12.7053	16.7053	AT1G63410; AT3G14260
	Seita.9G436900	0	2	2	0	12.5741	16.5741	AT2G30230; AT1G06980
<i>S. viridis</i>	Sevir.1G151100	2	0	2	0	13.2732	17.2732	AT1G12320; AT1G62840; AT3G60780; AT2G45360
	Sevir.5G247600	0	0	2	0	13.2732	15.2732	AT5G62770; AT3G27880; AT1G23710; AT1G70420

402 DATA ACCESS

403 JGI Plant Gene Atlas data are currently hosted at two portals: i) JGI Plant Gene Atlas
404 (<https://plantgeneatlas.jgi.doe.gov>), a dedicated portal provides bulk access to the data and user-specified
405 queries of a single gene to multiple gene sets, lets users access differentially expressed genes, visualize gene
406 ontology and pathway enrichments and track orthologs across the Gene Atlas plants; and ii) JGI's plant portal,
407 Phytozome (phytozome.jgi.doe.gov). Currently, Phytozome provides efficient tabular and graphical
408 representation of co-expressed genes, pathway details, peptide, CDS and transcript sequence, protein
409 homologs, plant family information and additionally genome browser view of gene models.

410

411 CONCLUSIONS

412 Here we analyzed the transcriptional landscape of 18 plants from 2,090 RNA-seq datasets. To the best of our
413 knowledge, it is the largest compendium of plant transcriptome data generated following standardized
414 protocols across diverse plant species. These datasets enable JGI's efforts to improve genome annotations
415 especially related to conserved biological processes across the diversity of plants. Comparing orthologs among
416 common gene sets between species allowed us to pinpoint and rank biologically relevant and evolutionarily
417 conserved genes, demonstrating the potential of cross-species analysis from the transcriptome resource
418 generated in this study. Furthermore, our results documented plant responses to varying N resources at the
419 organ level and expression variation among developmental stages. These and other analyses highlight shared
420 and varied gene expression regulatory evolution across plants.

421 The Gene Atlas datasets, along with the additional expression derived functional annotations, are valuable
422 resources to the plant research community and provide targets, unknown or poorly described TFs, hub genes,
423 and conserved genes, for functional studies that directly improve gene functional descriptions. We
424 acknowledge that these functional associations are not definitive evidence of their functions, but we anticipate
425 that they will be useful in directing future functional characterization experiments. We will continue to expand
426 the Gene Atlas through standardized procedures to increase the specificity of these function descriptions. We
427 strongly believe that results from this study and additional custom analyses on this resource will aid researchers
428 in better understanding of roles of genes in their own experiments and get a better handle on biological
429 processes at the system level.

430

431 METHODS

432 Plant growth and treatment conditions

433 ***Glycine max* and *Medicago truncatula*.** Plant seeds (*G. max* cv. Williams 82) were surface-sterilized, transferred to pots
434 containing 3:1 vermiculite perlite. 2/3 seedlings were planted in each pot and grown until plants were 4 weeks in a growth
435 chamber under 16 h-light/8 h-dark conditions, 26-23°C temperature maintained at 250 $\mu\text{mol m}^{-2}\text{s}^{-1}$. Plants for nitrogen
436 experiment were watered with nutrient solution containing either 10 mM KNO_3 (NO_3^- plants) or 10 mM $(\text{NH}_4)_3\text{PO}_4$ (NH_4^+ plants)
437 or 10 mM urea (urea plants). We selected urea as a control condition for the counter ions, potassium, and phosphate, as the
438 best compromise. The nutrient solutions were renewed every 3 days. After 4 weeks, different tissues (leaf, stem, root, shoot,
439 shoot tip, root tip, lateral roots, etc) for N regimes and standard conditions were harvested. Plants under symbiotic conditions
440 were watered with nutrient solution containing 0.5 mM NH_4NO_3 every other week. Subsequently, root nodules, roots, and
441 trifoliate leaves under symbiotic conditions were collected and tissues from flower open and un-open were harvested from
442 field grown plants.

443 ***Arabidopsis thaliana*.** Seeds were cold-stratified in water for 3 days and subsequently seeds were sown into 9 cm^2 plastic
444 pots (T.O. Plastics, Clearwater, FL, USA) filled with 2 parts Promix Biofungicide (Premier Tech, Rivière-du-Loup, QC, Canada)
445 to 1 part Profile Field and Fairway (Profile, Buffalo Grove, IL, USA). Pots were placed in a growth chamber (22°C days/20°C
446 nights, 14 h light at a photosynthetic photon flux density of 350 $\mu\text{mol m}^{-2}\text{s}^{-1}$), then thinned to 1 plant per pot containing
447 Sunshine MVP potting mix (SunGro Horticulture) and transferred into a greenhouse at the University of Texas at Austin when
448 rosettes had achieved 7-8 leaves. Plants supplemented with differing nitrogen source regimes (see *Glycine max*) were
449 harvested after 30 days.

450 ***Brachypodium distachyon*.** Seeds (*B. distachyon* Bd21) were grown in Metro mix 360 soil in a growth chamber, under 12 h
451 day and 12 h night conditions, maintained at 24°C/18°C, ~50% relative humidity; 150 $\mu\text{mol m}^{-2}\text{s}^{-1}$. Plants were watered once
452 a day or every two days depending on the size of plants and soil conditions and fertilized twice a week (Tuesday and Friday)
453 using Jack's 15-16-17 at a concentration of 100 ppm. For the nitrogen source study, plants grown for 30 days under differing
454 nitrogen source regimes (see *Glycine max*) were harvested.

455 For cold treatment experiment, Bd21 seeds were sown in soil without stratification. The germinated seeds were grown in a
456 growth chamber under short day conditions (26°C 10 h light, 18°C 14 h dark) for 4 weeks and then moved to a cold room

457 (4°C 10 h light, 4°C 14 h dark) for cold treatment. Whole shoots were harvested at different treatment time points and stored
458 at -80°C for RNA extraction.

459 ***Chlamydomonas reinhardtii***. *C. reinhardtii* strain CC-1690 (also known as 21gr) was cultured at 24°C (agitated at 180 rpm at
460 a photon flux density of 90 $\mu\text{mol m}^{-2}\text{s}^{-1}$ provided by cool white fluorescent bulbs at 4100 K and warm white fluorescent bulbs
461 at 3000 K used in the ratio of 2:1) in tris acetate-phosphate (TAP) medium (Boyle et al. 2012). For growth in differing nitrogen
462 sources, TAP medium was supplemented with $(\text{NH}_4)_3\text{PO}_4$ or KNO_3 , or urea (see *Glycine max*). Cultures of strain CC-1690 were
463 inoculated to 1×10^5 cells ml^{-1} and collected for RNA at 1×10^6 cells ml^{-1} , when the growth rates of all cultures were identical.
464 For assessing the impact of cell density, cultures were inoculated at 1×10^4 cells ml^{-1} in replete medium and sampled at $5 \times$
465 10^5 cells ml^{-1} and at each doubling thereafter until the culture reached a final density of 8×10^6 cells ml^{-1} .

466 ***Eucalyptus grandis***. *E. grandis* samples were derived from tissues collected from clonal ramets of the genotype BRASUZ1
467 that was used to generate the *E. grandis* reference genome. Tissue samples were collected from three trees ca. 5 years old,
468 and an adult tree ca. 8 years old at the time of sample collection, planted in experimental fields at Embrapa Genetic
469 Resources and Biotechnology in Brasilia, Brazil (15.73 South, 47.90 West). RNA samples were prepared from adult leaves
470 (completely developed), juvenile leaves (tender, thinner, not waxed), fruit buds, and developing cambium (from inside the tree
471 bark). Plant material was collected from the field, immediately frozen in liquid nitrogen, and stored at -80°C until RNA
472 extraction that followed an optimized CTAB-lithium chloride-based protocol (Ingliš et al. 2018).

473 ***Kalanchoë fedtschenkoi***. Four-week-old *K. fedtschenkoi* plants (accession ORNL M2) were grown under a 250 $\text{mmol m}^{-2} \text{s}^{-1}$
474 white light with a 12 h light (25°C)/12 h dark (18°C) cycle and were used as starting plant material for eight different
475 experiments (i.e., circadian, metabolite, temperature, drought, light intensity, light quality, nitrogen utilization, and standard
476 tissue). The experiments were conducted under day/night temperature regime of 25°C/18°C except the temperature
477 experiment. For the circadian experiment, two sets of plants were grown under a 12 h light/12 h dark cycle and continuous
478 lighting (250 $\text{mmol m}^{-2} \text{s}^{-1}$ white light), respectively, for seven days and then mature leaf samples (i.e., leaves 5-7 counting
479 from the top of the plants) were collected every two hours over a 48 h period. For the metabolite experiment, plants were
480 grown under an aerobic condition to prevent dark CO_2 fixation and malate accumulation. This was accomplished by putting
481 the plants in a sealed chamber with a closed air loop, through which air was continuously circulated. CO_2 was subsequently
482 continuously scrubbed from the air using a hydrated soda lime filter (LI-COR Biosciences, Lincoln NE) included in the loop.
483 CO_2 levels were monitored and maintained at an average of 3 ppm over the 12 h overnight aerobic treatment. Plants were
484 removed from the aerobic condition just prior to the start of the daylight photoperiod. Mature leaves were harvested at 2 h
485 intervals over the succeeding 24 h period (12 h light/12 h dark). For the temperature treatment, plants were grown under three
486 different temperatures (8°C, 25°C and 37°C), respectively, for seven days. For drought treatments, plants were grown under
487 three soil moisture conditions (40% \pm 3% [control], 20% \pm 3% [moderate drought] and 2% \pm 3% [severe drought]),
488 respectively, for 19 days. For the light intensity experiment, plants were grown under light intensity of 0 (darkness), 150 (low
489 light) and 1000 (high light) $\text{mmol m}^{-2} \text{s}^{-1}$ for 48 h. For the light quality experiment, plants were grown under blue light (270
490 $\text{mmol m}^{-2} \text{s}^{-1}$), red light (280 $\text{mmol m}^{-2} \text{s}^{-1}$), far-red light (280 $\text{mmol m}^{-2} \text{s}^{-1}$) and constant darkness for 48 h. For the nitrogen
491 utilization experiment, plants were treated with potassium sulfate (10 mM), ammonium sulfate (10 mM) and urea (5 mM),
492 respectively, for four weeks. Immediately after the temperature, drought, light intensity, light quality and nitrogen utilization
493 experiments, mature leaves were collected at two time points of dawn (2 h before the start of light period) and dusk (2 h
494 before the start of dark period). For the nitrogen utilization experiment, root samples were also collected at dawn and dusk,
495 respectively. For the standard tissue experiment, plants were grown in the greenhouse under a 12 h light/12 h dark cycle at
496 Oak Ridge National Laboratory (Oak Ridge, TN) and five different tissue types (young leaf, young stem, mature stem, root,
497 and flower) were collected at 10 am in the greenhouse.

498 ***Lupinus albus***. RNA-seq data from cluster root samples were obtained from (Hufnagel et al. 2020).

499 ***Panicum virgatum***. Vegetatively propagated Alamo AP13 plants were grown in pre-autoclaved MetroMix 300 substrate
500 (SunGro® Horticulture, <http://www.sunagro.com/>) and grown in a walk-in growth chamber at 30/26°C day/night temperature
501 with a 16 h photoperiod (250 $\mu\text{mol m}^{-2} \text{sec}^{-1}$) for four months. Tissues were harvested at six developmental stages, including leaf
502 development (VLD: V2), stem elongation (STE: E2 and E4), and reproductive phases (REP: R2, S2, and S6) (Moore et al.
503 1991).

504 For *P. virgatum* photoperiod experiment, four switchgrass genotypes, AP13, WBC, AP13, and VS16 plants were vegetatively
505 propagated and grown in one-gallon pots with a 6:1:1 mixture of Promix:Turface:Profile soil at a growth chamber at the
506 University of Texas at Austin. After one-week maintenance with a 30/25°C day/night temperature and 14L/10D photoperiod,
507 plants from each genotype were divided into two groups and received LD (16L/8D) or SD (8L/16D) treatment in separate
508 growth chambers. Fully emerged young leaves were simultaneously harvested from three individuals as three biological
509 replicates after three-week LD and SD treatments. We collected two leaf tissues (2cm leaf tips and 2 cm leaf base) at two
510 zeitgeber times (ZT1 and ZT17). All samples were immediately flash frozen in liquid nitrogen and stored at -80 °C for DNA and
511 RNA extraction.

512 ***Panicum hallii***. The *P. hallii* FIL2 (var. *filipes*; Corpus Christi, TX; 27.65° N, 97.40° W) and *P. hallii* HAL2 (var. *hallii*; Austin, TX;
513 30.19° N, 97.87° W) were grown in 3.78 L pots at the University of TX Brackenridge Field Laboratory (Austin, Texas) in the
514 greenhouse with mean daytime air temperature of 30°C and relative humidity of 65%. Plants supplemented with differing
515 nitrogen source regimes (see *Glycine max*) were harvested after 30 days.

516 For *P. hallii* panicle samples, genotypes, HAL2 and FIL2, were grown in a growth chamber at University of Texas at Austin
517 with 26°C day/22 °C night temperature and 12 h photoperiod. Plants were grown in 3.5 inches square pots with a 6:1:1
518 mixture of Promix:Turface:Profile soil. Young panicle tissues were collected under a dissection microscope and the

519 developmental stages were determined according to the lengths (0.1-0.2 cm for D1 stage, 0.5-1 cm for D2 stage, 4.5-5.5 cm
520 for D3 stage, and 9-11 cm for D4 stage). Tissues for D1 and D2 stages were taken from at least fifty plants and pooled for
521 each biological replicate. Tissues for D3 and D4 stages were taken from at least fifteen plants and pooled for each biological
522 replicate. All samples were harvested at 17:00-18:00 of the day and immediately flash frozen in liquid nitrogen. Three
523 biological replicates for each stage were stored at -80°C for DNA and RNA extraction.

524 ***Physcomitrium patens***. The protonemata cultures were systematically entrained by two successive weeks of culture prior to
525 treatment to obtain a homogeneous culture as described in Perroud *et al.* (Perroud *et al.* 2018). In brief, BCD (Cove *et al.*
526 2009) or Knop medium (Reski and Abel 1985) were used to culture the moss. Solid medium (medium with 1% [w/v] agar)
527 protonemal cultures were grown atop a cellophane film to allow tissue transfer for specific treatments (e.g., with hormones),
528 and for ease of harvesting. Plates and flasks were cultivated at 22°C with a 16 h-light/8 h-dark regime under 60-80 μmol
529 $\text{m}^{-2}\text{s}^{-1}$ white light (long-day conditions). All harvests were performed in the middle of the light photoperiod (+8 h of light in
530 long day conditions) (Perroud *et al.* 2018; Fernandez-Pozo *et al.* 2020).

531 ***Populus trichocarpa***. *Populus trichocarpa* (Nisqually-1) cuttings were potted in 4" X 4" X 5" containers containing 1:1 mix of
532 peat and perlite. Plants were grown under 16 h-light/8 h-dark conditions, maintained at 20-23°C and an average of 235 μmol
533 $\text{m}^{-2}\text{s}^{-1}$ to generate tissue for (1) standard tissues and (2) nitrogen source study. Plants for standard tissue experiment were
534 watered with McCown's woody plant nutrient solution and plants for nitrogen experiment were supplemented with either
535 10mM KNO_3 (NO_3^- plants) or 10mM $(\text{NH}_4)_3\text{PO}_4$ (NH_4^+ plants) or 10 mM urea (urea plants). Once plants reached leaf
536 plastochron index 15 (LPI-15), leaf, stem, root, and bud tissues were harvested and immediately flash frozen in liquid nitrogen
537 and stored at -80°C until further processing was done.

538 The plant material for the seasonal time course study was obtained from 2-year-old branches and apical buds (understood as
539 the top bud of each branch) of 5-year-old hybrid poplar (*Populus tremula* × *alba* INRA 717 1B4) trees planted at the Centre for
540 Plant Biotechnology and Genomics (CBGP) in Pozuelo de Alarcón, Madrid (3°49'W, 40°24'N), growing under natural
541 conditions. Stem samples were collected weekly from November 7, 2014, to April 9, 2015. Buds were collected weekly from
542 13 January to 14 April 2015. For each time point, stem portions from 8 trees and 25 apical buds from 8 trees were pooled.
543 RNA extraction was performed using the protocol described in (Ibañez *et al.* 2008). For the gene expression analysis, the
544 weekly data were divided into groups named; fall, winter, and spring. Letter suffixes - "a, b, c, d, e" were added to group
545 names representing "early," "mid," "late," "fortnight-1" or "fortnight-2" based on sampling dates within each season,
546 following the Northern Meteorological Seasons dates.

547 ***Setaria italica* and *Setaria viridis***. Seeds (*S. italica* B100 and *S. viridis* A10.1) were sown in flats (4x9 inserts/flat) containing
548 Metro mix 360 soil and grown in a growth chamber, under 12 h day and 12 h night conditions, maintained at 31°C/22°C,
549 50%-60% humidity; 450 $\mu\text{mol m}^{-2}\text{s}^{-1}$. Plants were watered once a day or every two days depending on the size of plants and
550 soil conditions and fertilized twice a week (Tuesday and Friday) using Jack's 15-16-17 at a concentration of 100 ppm. For
551 light treatment experiments, plants were grown under continuous monochromatic light, blue: 6 $\mu\text{mol m}^{-2}\text{s}^{-1}$, red: 50 $\mu\text{mol m}^{-2}\text{s}^{-1}$,
552 far-red: 80 $\mu\text{mol m}^{-2}\text{s}^{-1}$, respectively and watered with RO water every 3 days. Total aerial tissues were collected (at 9.30
553 AM) from 8-day old seedlings.

554 ***Sorghum bicolor***. The reference line BTx623 was grown under 14 h day greenhouse conditions in topsoil to generate tissue
555 for two separate experiments: (1) a nitrogen source study and (2) a tissue by developmental stage timecourse. For the
556 nitrogen source study, plants grown under differing nitrogen source regimes (see *Glycine max*) were harvested at 30 days
557 after emergence (DAE). For the tissue by developmental stage timecourse, plants were harvested at the juvenile stage (8
558 DAE), the vegetative stage (24 DAE), at floral initiation (44 DAE), at anthesis (65 DAE), and at grain maturity (96 DAE) and leaf,
559 root, stem and reproductive structures as described in McCormick *et al.* (McCormick *et al.* 2017).

560 ***Sorghum bicolor* var Rio**. Genetic material for *S. bicolor* var Rio was obtained from a single seed source provided by W.
561 Rooney at Texas A&M University. Plants were grown in greenhouse conditions and material for RNA extraction was collected
562 at 6 biological stages: vegetative (5-leaf), floral initiation, flag leaf, anthesis, soft dough, and hard dough. Stages were
563 identified based on biological characteristics defined in (Vanderlip and Reeves 1972). At every stage, whole plants were
564 harvested, and the topmost fully developed leaf and topmost internode were collected. During the first 3 stages, meristems
565 were isolated from the topmost internode while floral and seed tissues were collected after plants had flowered. All tissues
566 were immediately placed in RNA Later and stored at 4°C prior to RNA extraction. See also (Cooper *et al.* 2019).

567 ***Sphagnum angustifolium* (formally *S. fallax*)**. *S. angustifolium* were grown on BCD agar media pH 6.5, ambient temperature
568 (20°C) and 350 $\mu\text{mol m}^{-2}\text{s}^{-1}$ of photosynthetically active radiation (PAR) at a 12 h light/dark cycle for 2 months prior to
569 initiation of experimental conditions. At 8 am on the morning of the treatments, *Sphagnum* plantlets were transferred to petri
570 dishes with 15 ml of appropriate BCD liquid media and placed in a temperature-controlled growth cabinet. Excluding the dark
571 treatment, all samples were kept under 350 PAR for the duration of the experiment. Morning treatment samples were
572 harvested at noon. After each experiment the material was blotted dry, placed in a 15 mL Eppendorf tube, flash frozen in
573 liquid nitrogen, and stored at -80°C until RNA extractions were completed.

574 For the control treatment, *Sphagnum* plants were placed in a 22.05 cm^2 petri dish containing BCD media 6.5 pH and
575 incubated in a growth cabinet at 20°C and ambient light 350 PAR. To test low pH gene expression, the sample was placed in
576 a 22.05 cm^2 petri dish containing 6.5 pH BCD media at 8 AM. Each hour, the pH was gradually decreased until the sample
577 was transferred to 3.5 pH media at 11 AM. The samples were harvested at 12 PM. This treatment was repeated for the high
578 pH experiment except the sample was gradually brought from 6.5 to 9.0 pH. Temperature experiments were controlled in
579 growth cabinets plantlets in 22.05 cm^2 petri dishes containing 6.5 pH BCD media. The high temperature treatment began at
580 20°C and over three hours, temperature was gradually increased to 40°C. The low temperature treatment began at 20°C and

581 over three hours, was gradually decreased to 6°C. To test water loss effects on gene expression, plantlets were placed on dry
582 plates (no BCD media) for the duration of the experiment. Dark effect on gene expression was tested by placing plant
583 material in a BCD filled petri dish in complete darkness from 8 AM to 12 PM. To evaluate gene expression that is present
584 during immature growth stages, a sporophyte was collected from the mother of the *S. angustifolium* pedigree and germinated
585 on solid Knop medium under axenic tissue culture conditions. After 10 days of growth, plantlets were predominantly within
586 the thalloid protonemata with rhizoid stage and flash frozen in LN2 until RNA extraction using CTAB lysis buffer and Spectrum
587 Total Plant RNA kit.

588 **RNA extraction and sequencing**

589 All tissues were immediately flash frozen in liquid nitrogen and stored at -80°C until further processing was done. Every
590 harvest involved at least three independent biological replicates for each condition. High quality RNA was extracted mainly
591 using standard Trizol-reagent based extraction (Z. Li and Trick 2005), exceptions noted above under individual species. The
592 integrity and concentration of the RNA preparations were checked initially using Nano-Drop ND-1000 (Nano-Drop
593 Technologies) and then by BioAnalyzer (Agilent Technologies). Plate-based RNA sample prep was performed on the
594 PerkinElmer Sciclone NGS robotic liquid handling system using Illumina's TruSeq Stranded mRNA HT sample prep kit utilizing
595 poly-A selection of mRNA following the protocol outlined by Illumina in their user guide:
596 http://support.illumina.com/sequencing/sequencing_kits/truseq_stranded_mrna_ht_sample_prep_kit.html, and with the
597 following conditions: total RNA starting material was 1 µg per sample and 8 cycles of PCR was used for library amplification.
598 The prepared libraries were then quantified by qPCR using the Kapa SYBR Fast Illumina Library Quantification Kit (Kapa
599 Biosystems) and run on a Roche LightCycler 480 real-time PCR instrument. The quantified libraries were then prepared for
600 sequencing on the Illumina HiSeq sequencing platform utilizing a TruSeq paired-end cluster kit, v4, and Illumina's cBot
601 instrument to generate a clustered flow cell for sequencing. Sequencing of the flow cell was performed on the Illumina
602 HiSeq2500 sequencer using HiSeq TruSeq SBS sequencing kits, v4, following a 2x150 indexed run recipe. The same
603 standardized protocols were used to prevent introduction of any batch effects among samples throughout the project.
604

605 **RNA-seq data normalization and differential gene expression analysis**

606 Illumina RNA-seq 150 bp paired-end strand-specific reads were processed using custom Python scripts to trim adapter
607 sequences and low-quality bases to obtain high quality (Q_≥25) sequence data. Reads shorter than 50 bp after trimming were
608 discarded. The processed high-quality RNA-seq reads were aligned to current reference genomes of Gene Atlas using
609 GSNAP, a short read alignment program (Wu and Nacu 2010). HTSeq v1.99.2, a Python package was used to count reads
610 mapped to annotated genes in the reference genome (Anders, Pyl, and Huber 2015).
611 Multiple steps for vetting libraries and identifying outliers were employed, including visualizing the multidimensional scaling
612 plots to identify batch effects, if any, and outliers among the biological replicates were further identified based on Euclidean
613 distance to the cluster center and the Pearson correlation coefficient, $r \geq 0.85$. Libraries retained after QC and outlier-filtering
614 steps were only considered for further analysis. Detected batch effects, if any, were accounted for using RUVSeq (v1.4.0)
615 (Risso et al. 2014) with the residual RUVr approach. Fragments per kilobase of exon per million fragments mapped (FPKM)
616 and transcripts per million (TPM) values were calculated for each gene by normalizing the read count data to both the length
617 of the gene and the total number of mapped reads in the sample and considered as the metric for estimating gene expression
618 levels (B. Li and Dewey 2011; Trapnell et al. 2011). Genes with low expression were filtered out, by requiring ≥ 2 relative log
619 expression normalized counts in at least two samples for each gene. Differential gene expression analysis was performed
620 using the DESeq2 package (v1.30.1) (Love, Huber, and Anders 2014) with adjusted *P*-value < 0.05 using the Benjamini &
621 Hochberg method and an \log_2 fold change > 1 as the statistical cutoff for differentially expressed genes.
622

623 **Co-expression network construction**

624 Weighted gene co-expression networks were constructed using the WGCNA R package (v1.70.3) (Langfelder and Horvath
625 2008) with normalized expression data retained after filtering genes showing low expression levels (\log_2 values of expression
626 < 2). Subsets of samples belonging to specific experiments such as N study, developmental stages, or stress treatment, were
627 used to construct multiple networks for each species. Subsetting samples reduces the noise and increases the functional
628 connectivity and specificity within modules. We followed standard WGCNA network construction procedures for this analysis.
629 Briefly, pairwise Pearson correlations between each gene pair was weighted by raising them to power (β). To select proper
630 soft-thresholding power, the network topology for a range of powers was evaluated and appropriate power was chosen that
631 ensured an approximate scale-free topology of the resulting network. The pairwise weighted matrix was transformed into a
632 topological overlap measure (TOM). And the TOM-based dissimilarity measure (1 - TOM) was used for hierarchical clustering
633 and initial module assignments were determined by using a dynamic tree-cutting algorithm. Pearson correlations between
634 each gene and each module eigengene, referred to as a gene's module membership, were calculated and module eigengene
635 distance threshold of 0.25 was used to merge highly similar modules. These co-expression modules were assessed to
636 determine their association with expression patterns distinct to a tissue or condition. Module eigengenes were associated
637 with tissues or treatment conditions or developmental stages to gain insight into the role each module might play. These
638 modules were visualized using igraph R package (v.1.2.6) (Gabor Csardi and Tamas Nepusz 2006) and in order to focus on
639 relevant gene pair relationships, network depictions were limited to top 500 within-module gene-gene interactions as
640 measured by topological overlap.
641

642 **GO and KEGG pathway enrichment analysis**

643 GO enrichment analysis of DEGs, co-expression modules and genes in tissue and condition specific clusters was performed
644 using topGO (v.2.42.0) (Alexa A and Rahnenfuhrer J 2016), an R Bioconductor package, to determine overrepresented GO
645 categories across biological process (BP), cellular component (CC) and molecular function (MF) domains. Enrichment of GO
646 terms was tested using Fisher's exact test with *P* < 0.05 considered as significant. KEGG (Kanehisa and Goto 2000) pathway
647

648 enrichment analysis was also performed on those gene sets based on hypergeometric distribution tests and pathways with P
649 <0.05 were considered as enriched.

650

651 **Categorization of function descriptions**

652 An augmented dictionary lookup approach that incorporates weighting for positive (amplifiers), negative (including
653 attenuators), and adversative keywords was adapted from sentiment analysis methodology to categorize gene function
654 descriptions. We generated a custom dictionary from gene function descriptions of all Gene Atlas plants and used a modified
655 valence shifters data table with sentimentr (v.2.9.0) (<https://cran.r-project.org/web/packages/sentimentr/>), to obtain sentiment
656 score. We empirically determined the minimum cutoff for sentiment score to classify gene descriptions as good (score > 0.3)
657 and poor (score < 0.3) function descriptors.

658

659 **Identification of orthologous genes**

660 OrthoFinder (v2.5.4) was used to identify orthologous genes across 18 Gene Atlas species using default parameters (Emms
661 and Kelly 2019). OrthoFinder results were parsed to generate tables of orthologs for each species and genes with one-to-one
662 ortholog relationships between species identified using rooted gene trees were further subsetted.

663

664 **Gene ranking method**

665 To rank and prioritize genes by their biological relevance, genes with distinct expression patterns identified based on i)
666 tissue/condition specificity, ii) unique DE in a single contrast were given a score of 2 for each method i.e., a gene was
667 assigned a score of 4 if it were identified by two methods. These scores were augmented with co-expression network
668 analysis (described above). Genes in biologically relevant modules were ranked (score=2) while hub genes in a co-expression
669 module were ranked the highest (score=4). Also, gene orthologs with consensus expression pattern in two or more plants
670 were given additional scores based on the phylogenetic distance between species (Zeng et al. 2014; Kumar et al. 2017) i.e.,
671 larger the divergence time higher the score (million years ago/100) (**Supplemental Data 16**). Final ranking of the genes was
672 calculated as the aggregate of individual scores.

673

674 **System design and implementation**

675 All statistical analyses and visualizations were performed using the R 4.0.3 Statistical Software (R Development Core Team
676 2011) and its web interface was developed using shiny (v1.7.1). Currently, Gene Atlas is deployed on a CentOS Linux server
677 by employing Docker (version 19.03.11), an open platform for developing and running applications.

678

679 **Data availability**

680 The RNA-seq data that support the findings of this study are available from the NCBI Sequence Read Archive (SRA) under
681 accessions provided in **Supplemental Data 1**. To enable exploration of the transcriptome datasets for JGI Plant Gene Atlas
682 v2.0, the data are hosted on Gene Atlas portal (<https://plantgeneatlas.jgi.doe.gov>) and JGI's Phytosome plant portal.
683 Documentation for data processing and downloadable data are available in the 'Methods' section
684 (<https://plantgeneatlas.jgi.doe.gov>).

685

686

687 **Competing financial interests**

688 The authors declare no competing financial interests.

689

690

691 **Correspondence and requests for materials** should be addressed to A.S. or J.S.

692

693

694 **ACKNOWLEDGMENTS**

695 The work (proposal: 10.46936/10.25585/60000843) conducted by the U.S. Department of Energy Joint Genome Institute
696 (<https://ror.org/04xm1d337>), a DOE Office of Science User Facility, is supported by the Office of Science of the U.S.
697 Department of Energy operated under Contract No. DE-AC02-05CH11231.

698

699 The *Populus* work was partially supported by the U.S. Department of Energy under Contract to Oak Ridge National
700 Laboratory. Oak Ridge National Laboratory is managed by UT-Battelle, LLC for the US Department of Energy under contract
701 number DE- DE-AC05-00OR22725. Specific funding for the soybean transcriptome atlas was provided by a grant from the
702 United Soybean Board (to GS). The switchgrass work was carried out under the support of the BioEnergy Science Center
703 (BESC, a U.S. Department of Energy Bioenergy Research Center supported by the Office of Biological and Environmental
704 Research in the DOE Office of Science, U.S. Department of Energy) and funded by the Samuel Roberts Noble Foundation. BH
705 work was funded in part by U.S. DOE the Office of Biological and Environmental Research under grant number DE-
706 SC0012629. The *Chlamydomonas* work is supported by the US Department of Energy Grant DE-FC02-02ER63421 and by the
707 National Institutes of Health (NIH) R24 GM092473 to SM. The Eucalyptus work was supported by the Brazilian Federal District
708 Research Foundation (FAP-DF) NEXTREE grant. The *Panicum hallii* work was supported by the DOE Office of Science, Office
709 of Biological and Environmental Research (BER), grant no. DE-SC0008451 and DE-SC0021126 to TEJ. The sorghum work by
710 JM laboratory was funded in part by the DOE Great Lakes Bioenergy Research Center (DOE BER grant DE-SC0018409). The
711 *Setaria* work was funded by the DOE Office of Science under grant numbers DE-SC0018277 and DE-SC0008769. The
712 *Kalanchoë* work was partially supported by the DOE Office of Science, Genomic Science Program under Award No. DE-
713 SC0008834. Research related to Sphagnum was funded by DOE BER Early Career Research Program at Oak Ridge National

Sreedasyam et al. 2022 (preprint) JGI Plant Gene Atlas

714 Laboratory is managed by UT-Battelle, LLC, for the US DOE under contract number DE-AC05-00OR22725. Thanks to Daniel
715 S. Rokhsar for involvement in the early formulation of Gene Atlas and helpful discussions.

716

717 AUTHOR CONTRIBUTIONS

718 A.S. and C.P. conducted transcriptome data analyses. J.T.L. conducted metadata analysis. MSH carried out soybean and
719 *Medicago* experiments. J.G., K.B., M.A., M.K., M.W., A.L., Jenifer J, L.S., K.A., M.Z., C.D. performed RNA-seq library
720 preparation and sequencing. J.K. and S.D.G. conducted *Chlamydomonas* experiments. J.C., J.P., and D.G. maintains the
721 data repository at Phytozome. J.W.J. and C.P. assembled genomes. S.S. conducted genome annotation at JGI. I.T.-J., and
722 M.U. conducted *Panicum virgatum* experiments. S.S.J. conducted *Populus* experiments and *Sphagnum* RNA extractions.
723 D.C. and M.P. conducted *Populus* seasonal time course experiments. H.J., C.S., P.H., J.S., C.L., A.M. and S.C. conducted
724 *Setaria* experiments and sample preparations. L.L. conducted Brachypodium cold treatment experiments. A.A.C. conducted
725 *Sphagnum* experiments. B.W. conducted *Sorghum* N-treatment experiments. R.H. conducted *Kalanchoe* experiments. M.R.P.
726 conducted *Eucalyptus* experiments. R.T. and K.S. conducted validation experiments for N-treatment. E.V.S. and X.W.
727 conducted Arabidopsis, *P. hallii* and *P. virgatum* photoperiod experiments and sample preparations. A.M. conducted *P.*
728 *virgatum* drought stress experiments and sample preparation. P.F.P. and F.B.H. analyzed *Physcomitrium* data. P.F.P., M.H.
729 and S.A.R. provided *Physcomitrium* samples. D.S.R., D.G., D.T., D.W., E.A.C., E.K., G.S., G.A.T., I.B., J.S., J.M., J.V., S.A.R.,
730 S.S.M., T.B., T.E.J., T.C.M., X.Y., and Y.T. are principal investigators (alphabetical order). All authors read and approved the
731 final manuscript.
732 A.S., J.T.L., and J.S. prepared the manuscript with input from all authors.

733

734

735 SUPPLEMENTAL MATERIAL

736 **Supplemental Data 1.** Correlation among biological replicates in Gene Atlas species.

737 **Supplemental Data 2.** RNA-seq samples generated/analyzed in this study.

738 **Supplemental Data 3.** One-to-one orthologous genes across eight vascular plants.

739 **Supplemental Data 4.** One-to-one orthologous genes with consistent expression among species, but weak functional
740 descriptions.

741 **Supplemental Data 5.** *Arabidopsis thaliana* (TAIR10) orthologs of genes with conserved expression patterns across Gene
742 Atlas plants.

743 **Supplemental Data 6.** Percentage of genes commonly expressed in multiple tissues in Gene Atlas plants.

744 **Supplemental Data 7.** Genes with strong expression proclivity towards selected tissues/conditions in *G. max*, *P. patens* and
745 *S. angustifolium*.

746 **Supplemental Data 8.** Genes with strong tissue/condition specific expression across Gene Atlas plants.

747 **Supplemental Data 9.** Overrepresented biological processes among genes with strong tissue/condition specific expression.

748 **Supplemental Data 10.** Differentially expressed genes in nitrogen treatment study.

749 **Supplemental Data 11.** Co-expression network module genes generated across different sets of tissues and conditions
750 within Gene Atlas plants.

751 **Supplemental Data 12.** Overrepresented biological processes among co-expression network module gene sets generated
752 across different sets of tissues and conditions within Gene Atlas plants.

753 **Supplemental Data 13.** List of hub genes in co-expression network modules.

754 **Supplemental Data 14.** Expression derived function descriptions (EDFD) assigned to annotated genes across Gene Atlas
755 plants.

756 **Supplemental Data 15.** Prioritized top ranked genes with poor functional descriptions for future experimental investigations.

757 **Supplemental Data 16.** Estimates of divergence time between Gene Atlas species.

758

759

760

760 REFERENCES

761 Alexa A and Rahnenfuhrer J. 2016. "topGO: Enrichment Analysis for Gene Ontology." R Package Version 2.24.0. 2016.
762 <http://bioconductor.org/packages/release/bioc/html/topGO.html>.

763 Anders, Simon, Paul Theodor Pyl, and Wolfgang Huber. 2015. "HTSeq-A Python Framework to Work with High-Throughput
764 Sequencing Data." *Bioinformatics* 31 (2): 166-69.

765 Berardini, Tanya Z., Leonore Reiser, Donghui Li, Yarik Mezheritsky, Robert Muller, Emily Strait, and Eva Huala. 2015. "The
766 Arabidopsis Information Resource: Making and Mining the 'Gold Standard' Annotated Reference Plant Genome."

- 767 *Genesis* 53 (8): 474–85.
- 768 Bruex, Angela, Raghunandan M. Kainkaryam, Yana Wieckowski, Yeon Hee Kang, Christine Bernhardt, Yang Xia, Xiaohua
769 Zheng, et al. 2012. “A Gene Regulatory Network for Root Epidermis Cell Differentiation in Arabidopsis.” *PLoS Genetics*
770 8 (1). <https://doi.org/10.1371/journal.pgen.1002446>.
- 771 Canales, Javier, Tomás C. Moyano, Eva Villarroel, and Rodrigo A. Gutiérrez. 2014. “Systems Analysis of Transcriptome Data
772 Provides New Hypotheses about Arabidopsis Root Response to Nitrate Treatments.” *Frontiers in Plant Science* 5: 22.
- 773 Cooper, Elizabeth A., Zachary W. Brenton, Barry S. Flinn, Jerry Jenkins, Shengqiang Shu, Dave Flowers, Feng Luo, et al.
774 2019. “A New Reference Genome for Sorghum Bicolor Reveals High Levels of Sequence Similarity between Sweet and
775 Grain Genotypes: Implications for the Genetics of Sugar Metabolism.” *BMC Genomics* 20 (1): 420.
- 776 Cove, David J., Pierre-François Perroud, Audra J. Charron, Stuart F. McDaniel, Abha Khandelwal, and Ralph S. Quatrano.
777 2009. “The Moss *Physcomitrella Patens*: A Novel Model System for Plant Development and Genomic Studies.” *Cold*
778 *Spring Harbor Protocols* 2009 (2): db.emo115.
- 779 Emms, David M., and Steven Kelly. 2019. “OrthoFinder: Phylogenetic Orthology Inference for Comparative Genomics.”
780 *Genome Biology* 20 (1): 238.
- 781 Faye, Jacques M., Eyanawa A. Akata, Bassirou Sine, Cyril Diatta, Ndiaga Cisse, Daniel Fonceka, and Geoffrey P. Morris.
782 2022. “Quantitative and Population Genomics Suggest a Broad Role of Stay-Green Loci in the Drought Adaptation of
783 Sorghum.” *The Plant Genome* 15 (1): e20176.
- 784 Fernandez-Pozo, N., F. B. Haas, R. Meyberg, K. K. Ullrich, M. Hiss, P-F Perroud, S. Hanke, et al. 2020. “PEATmoss
785 (*Physcomitrella* Expression Atlas Tool): A Unified Gene Expression Atlas for the Model Plant *Physcomitrella Patens*.”
786 *The Plant Journal: For Cell and Molecular Biology* 102 (1). <https://doi.org/10.1111/tpj.14607>.
- 787 Gabor Csardi and Tamas Nepusz. 2006. “The Igraph Software Package for Complex Network Research.” *InterJournal,*
788 *Complex Systems*. 2006. <http://igraph.org>.
- 789 Gelli, Malleswari, Yongchao Duo, Anji Konda, Chi Zhang, David Holding, Ismail Dweikat, A. B. Maunder, et al. 2014.
790 “Identification of Differentially Expressed Genes between Sorghum Genotypes with Contrasting Nitrogen Stress
791 Tolerance by Genome-Wide Transcriptional Profiling.” *BMC Genomics* 15 (1): 179.
- 792 Ghazalpour, Anatole, Sudheer Doss, Bin Zhang, Susanna Wang, Christopher Plaisier, Ruth Castellanos, Alec Brozell, et al.
793 2006. “Integrating Genetic and Network Analysis to Characterize Genes Related to Mouse Weight.” *PLoS Genetics* 2
794 (8): e130.
- 795 Gollery, Martin, Jeff Harper, John Cushman, Taliah Mittler, Thomas Girke, Jian-Kang Zhu, Julia Bailey-Serres, et al. 2006.
796 “What Makes Species Unique? The Contribution of Proteins with Obscure Features.” *Genome Biology* 7 (7): R57.
- 797 Gollery, Martin, Jeff Harper, John Cushman, Taliah Mittler, and Ron Mittler. 2007. “POFs: What We Don’t Know Can Hurt Us.”
798 *Trends in Plant Science* 12 (11): 492–96.
- 799 Goodstein, David M., Shengqiang Shu, Russell Howson, Rochak Neupane, Richard D. Hayes, Joni Fazo, Therese Mitros, et
800 al. 2012. “Phytozome: A Comparative Platform for Green Plant Genomics.” *Nucleic Acids Research* 40 (D1): 1–9.
- 801 Horvath, S., B. Zhang, M. Carlson, K. V. Lu, S. Zhu, R. M. Felciano, M. F. Lurance, et al. 2006. “Analysis of Oncogenic
802 Signaling Networks in Glioblastoma Identifies ASPM as a Molecular Target.” *Proceedings of the National Academy of*
803 *Sciences of the United States of America* 103 (46): 17402–7.
- 804 Huang, Jianyan, Xiaobo Zhao, and Joanne Chory. 2019. “The Arabidopsis Transcriptome Responds Specifically and
805 Dynamically to High Light Stress.” *Cell Reports* 29 (12): 4186–99.e3.
- 806 Hufnagel, Bárbara, André Marques, Alexandre Soriano, Laurence Marquès, Fanchon Divol, Patrick Dumas, Erika Sallet, et al.
807 2020. “High-Quality Genome Sequence of White Lupin Provides Insight into Soil Exploration and Seed Quality.” *Nature*
808 *Communications*. <https://doi.org/10.1038/s41467-019-14197-9>.
- 809 Ibañez, Cristian, Alberto Ramos, Paloma Acebo, Angela Contreras, Rosa Casado, Isabel Allona, and Cipriano Aragoncillo.
810 2008. “Overall Alteration of Circadian Clock Gene Expression in the Chestnut Cold Response.” *PLoS One* 3 (10): e3567.
- 811 Inglis, Peter W., Marilia de Castro R. Pappas, Lucileide V. Resende, and Dario Grattapaglia. 2018. “Fast and Inexpensive
812 Protocols for Consistent Extraction of High Quality DNA and RNA from Challenging Plant and Fungal Samples for High-
813 Throughput SNP Genotyping and Sequencing Applications.” *PLoS One* 13 (10): e0206085.
- 814 Jin, Jinpu, Feng Tian, De-Chang Yang, Yu-Qi Meng, Lei Kong, Jingchu Luo, and Ge Gao. 2017. “PlantTFDB 4.0: Toward a
815 Central Hub for Transcription Factors and Regulatory Interactions in Plants.” *Nucleic Acids Research* 45 (D1): D1040–
816 45.
- 817 Kanehisa, M., and S. Goto. 2000. “KEGG: Kyoto Encyclopedia of Genes and Genomes.” *Nucleic Acids Research* 28 (1): 27–
818 30.
- 819 Keightley, Peter D., and William George Hill. 1990. “Variation Maintained in Quantitative Traits with Mutation–selection

- 820 Balance: Pleiotropic Side-Effects on Fitness Traits." *Proceedings of the Royal Society of London. Series B: Biological*
821 *Sciences* 242 (1304): 95–100.
- 822 Kogawara, Satoshi, Takashi Yamanoshita, Mariko Norisada, and Katsumi Kojima. 2014. "Steady Sucrose Degradation Is a
823 Prerequisite for Tolerance to Root Hypoxia." *Tree Physiology* 34 (3): 229–40.
- 824 Koornneef, Maarten, and David Meinke. 2010. "The Development of Arabidopsis as a Model Plant." *The Plant Journal: For*
825 *Cell and Molecular Biology* 61 (6): 909–21.
- 826 Kryuchkova-Mostacci, Nadezda, and Marc Robinson-Rechavi. 2017. "A Benchmark of Gene Expression Tissue-Specificity
827 Metrics." *Briefings in Bioinformatics* 18 (2): 205–14.
- 828 Kumar, Sudhir, Glen Stecher, Michael Suleski, and S. Blair Hedges. 2017. "TimeTree: A Resource for Timelines, Timetrees,
829 and Divergence Times." *Molecular Biology and Evolution* 34 (7): 1812–19.
- 830 Langfelder, Peter, and Steve Horvath. 2008. "WGCNA: An R Package for Weighted Correlation Network Analysis." *BMC*
831 *Bioinformatics* 9 (January): 559.
- 832 Levin, J. Z., M. Yassour, X. Adiconis, C. Nusbaun, D. A. Thompson, N. Friedman, A. Gnirke, and A. Regev. 2010.
833 "Comprehensive Comparative Analysis of Strand Specific RNA Sequencing Methods." *Nature Methods* 7 (9): 709–15.
- 834 Li, Bo, and Colin N. Dewey. 2011. "RSEM: Accurate Transcript Quantification from RNA-Seq Data with or without a Reference
835 Genome." *BMC Bioinformatics* 12 (1): 323.
- 836 Li, Chun, Qi Gang Li, Jim M. Dunwell, and Yuan Ming Zhang. 2012. "Divergent Evolutionary Pattern of Starch Biosynthetic
837 Pathway Genes in Grasses and Dicots." *Molecular Biology and Evolution* 29 (10): 3227–36.
- 838 Liu, Wenwen, Guangming He, and Xing Wang Deng. 2021. "Biological Pathway Expression Complementation Contributes to
839 Biomass Heterosis in Arabidopsis." *Proceedings of the National Academy of Sciences of the United States of America*
840 118 (16): e2023278118.
- 841 Li, W., P. Lan, and 3.948. 2015. "Re-Analysis of RNA-Seq Transcriptome Data Reveals New Aspects of Gene Activity in
842 Arabidopsis Root Hairs." *Frontiers in Plant Science* 6 (June): 421.
- 843 Li, Yinruizhi, Mengdi Wang, Ke Teng, Di Dong, Zhuocheng Liu, Tiejun Zhang, and Liebao Han. 2022. "Transcriptome Profiling
844 Revealed Candidate Genes, Pathways and Transcription Factors Related to Nitrogen Utilization and Excessive Nitrogen
845 Stress in Perennial Ryegrass." *Scientific Reports* 12 (1): 3353.
- 846 Li, Zhiwu, and Harold N. Trick. 2005. "Rapid Method for High-Quality RNA Isolation from Seed Endosperm Containing High
847 Levels of Starch." *BioTechniques* 38 (6): 872, 874, 876.
- 848 Loreti, Elena, Alessandra Poggi, Giacomo Novi, Amedeo Alpi, and Pierdomenico Perata. 2005. "A Genome-Wide Analysis of
849 the Effects of Sucrose on Gene Expression in Arabidopsis Seedlings under Anoxia." *Plant Physiology* 137 (3): 1130–38.
- 850 Love, Michael I., Wolfgang Huber, and Simon Anders. 2014. "Moderated Estimation of Fold Change and Dispersion for RNA-
851 Seq Data with DESeq2." *Genome Biology* 15 (12): 550.
- 852 Ma, Fei, Lijuan Wang, Jiale Li, Muhammad Kaleem Samma, Yanjie Xie, Ren Wang, Jin Wang, Jing Zhang, and Wenbiao Shen.
853 2014. "Interaction between HY1 and H2O2 in Auxin-Induced Lateral Root Formation in Arabidopsis." *Plant Molecular*
854 *Biology* 85 (1-2): 49–61.
- 855 Manzano, Concepción, Mercedes Pallero-Baena, Ilda Casimiro, Bert De Rybel, Beata Orman-Ligeza, Gert Van Isterdael, Tom
856 Beeckman, Xavier Draye, Pedro Casero, and Juan C. Del Pozo. 2014. "The Emerging Role of Reactive Oxygen Species
857 Signaling during Lateral Root Development." *Plant Physiology* 165 (3): 1105–19.
- 858 McCormick, R. F., S. K. Truong, A. Sreedasyam, J. Jenkins, S. Shu, D. Sims, M. Kennedy, et al. 2017. "The Sorghum Bicolor
859 Reference Genome: Improved Assembly, Gene Annotations, a Transcriptome Atlas, and Signatures of Genome
860 Organization." *The Plant Journal: For Cell and Molecular Biology*. <https://doi.org/10.1111/tpj.13781>.
- 861 Miller, Jeremy A., Michael C. Oldham, and Daniel H. Geschwind. 2008. "A Systems Level Analysis of Transcriptional Changes
862 in Alzheimer's Disease and Normal Aging." *The Journal of Neuroscience: The Official Journal of the Society for*
863 *Neuroscience* 28 (6): 1410–20.
- 864 Mukhtar, M. Shahid, Anne-Ruxandra Carvunis, Matija Dreze, Petra Epple, Jens Steinbrenner, Jonathan Moore, Murat Tasan,
865 et al. 2011. "Independently Evolved Virulence Effectors Converge onto Hubs in a Plant Immune System Network."
866 *Science* 333 (6042): 596–601.
- 867 Nicotra, A. B., O. K. Atkin, S. P. Bonser, A. M. Davidson, E. J. Finnegan, U. Mathesius, P. Poot, et al. 2010. "Plant Phenotypic
868 Plasticity in a Changing Climate." *Trends in Plant Science*. <https://doi.org/10.1016/j.tplants.2010.09.008>.
- 869 Passaia, Gisele, Guillaume Queval, Juan Bai, Marcia Margis-Pinheiro, and Christine H. Foyer. 2014. "The Effects of Redox
870 Controls Mediated by Glutathione Peroxidases on Root Architecture in Arabidopsis Thaliana." *Journal of Experimental*
871 *Botany* 65 (5): 1403–13.
- 872 Peña, María J., Yingzhen Kong, William S. York, and Malcolm A. O'Neill. 2012. "A Galacturonic Acid-Containing Xyloglucan Is

- 873 Involved in Arabidopsis Root Hair Tip Growth.” *The Plant Cell* 24 (11): 4511–24.
- 874 Perroud, Pierre-François, Fabian B. Haas, Manuel Hiss, Kristian K. Ullrich, Alessandro Alboresi, Mojgan Amirebrahimi, Kerrie
875 Barry, et al. 2018. “The Physcomitrella Patens Gene Atlas Project: Large-Scale RNA-Seq Based Expression Data.” *The*
876 *Plant Journal: For Cell and Molecular Biology* 95 (1): 168–82.
- 877 Raissig, Michael T., Juliana L. Matos, M. Ximena Anleu Gil, Ari Kornfeld, Akhila Bettadapur, Emily Abrash, Hannah R. Allison,
878 et al. 2017. “Mobile MUTE Specifies Subsidiary Cells to Build Physiologically Improved Grass Stomata.” *Science* 355
879 (6330): 1215–18.
- 880 Reski, R., and W. O. Abel. 1985. “Induction of Budding on Chloronemata and Caulonemata of the Moss, Physcomitrella
881 Patens, Using Isopentenyladenine.” *Planta* 165 (3): 354–58.
- 882 Rhee, Seung Yon, and Marek Mutwil. 2014. “Towards Revealing the Functions of All Genes in Plants.” *Trends in Plant*
883 *Science* 19 (4): 212–21.
- 884 Risso, Davide, John Ngai, Terence P. Speed, and Sandrine Dudoit. 2014. “Normalization of RNA-Seq Data Using Factor
885 Analysis of Control Genes or Samples (RUVSeq).” *Nature Biotechnology* 32 (9): 896–902.
- 886 Ross, Michael G., Carsten Russ, Maura Costello, Andrew Hollinger, Niall J. Lennon, Ryan Hegarty, Chad Nusbaum, et al.
887 2013. “Characterizing and Measuring Bias in Sequence Data.” *Genome Biology* 14 (5): R51.
- 888 Somssich, Marc, Ghazanfar Abbas Khan, and Staffan Persson. 2016. “Cell Wall Heterogeneity in Root Development of
889 Arabidopsis.” *Frontiers in Plant Science* 7 (August): 1242.
- 890 Sudmant, Peter H., Maria S. Alexis, and Christopher B. Burge. 2015. “Meta-Analysis of RNA-Seq Expression Data across
891 Species, Tissues and Studies.” *Genome Biology* 16 (1): 287.
- 892 Swift, Joseph, Jose M. Alvarez, Viviana Araus, Rodrigo A. Gutiérrez, and Gloria M. Coruzzi. 2020. “Nutrient Dose-Responsive
893 Transcriptome Changes Driven by Michaelis–Menten Kinetics Underlie Plant Growth Rates.” *Proceedings of the*
894 *National Academy of Sciences* 117 (23): 12531–40.
- 895 Torkamani, Ali, Brian Dean, Nicholas J. Schork, and Elizabeth A. Thomas. 2010. “Coexpression Network Analysis of Neural
896 Tissue Reveals Perturbations in Developmental Processes in Schizophrenia.” *Genome Research* 20 (4): 403–12.
- 897 Trapnell, Cole, Brian a. Williams, Geo Pertea, Ali Mortazavi, Gordon Kwan, Marijke J. van Baren, Steven L. Salzberg, Barbara
898 J. Wold, and Lior Pachter. 2011. “Transcript Assembly and Abundance Estimation from RNA-Seq Reveals Thousands
899 of New Transcripts and Switching among Isoforms.” *Nature Biotechnology* 28 (5): 511–15.
- 900 Vanderlip, R. L., and H. E. Reeves. 1972. “Growth Stages of Sorghum [*Sorghum Bicolor* , (L.) Moench.] 1.” *Agronomy Journal*
901 64 (1): 13–16.
- 902 Voineagu, Irina, Xinchun Wang, Patrick Johnston, Jennifer K. Lowe, Yuan Tian, Steve Horvath, Jonathan Mill, Rita M. Cantor,
903 Benjamin J. Blencowe, and Daniel H. Geschwind. 2011. “Transcriptomic Analysis of Autistic Brain Reveals Convergent
904 Molecular Pathology.” *Nature* 474 (7351): 380–84.
- 905 Wu, Thomas D., and Serban Nacu. 2010. “Fast and SNP-Tolerant Detection of Complex Variants and Splicing in Short
906 Reads.” *Bioinformatics* 26 (7): 873–81.
- 907 Yanai, Itai, Hila Benjamin, Michael Shmoish, Vered Chalifa-Caspi, Maxim Shklar, Ron Ophir, Arren Bar-Even, et al. 2005.
908 “Genome-Wide Midrange Transcription Profiles Reveal Expression Level Relationships in Human Tissue Specification.”
909 *Bioinformatics* 21 (5): 650–59.
- 910 Yu, Y., J. C. Fuscoe, C. Zhao, C. Guo, M. Jia, T. Qing, D. I. Bannon, et al. 2014. “A Rat RNA-Seq Transcriptomic BodyMap
911 across 11 Organs and 4 Developmental Stages.” *Nature Communications* 5: 3230.
- 912 Zeng, Liping, Qiang Zhang, Renran Sun, Hongzhi Kong, Ning Zhang, and Hong Ma. 2014. “Resolution of Deep Angiosperm
913 Phylogeny Using Conserved Nuclear Genes and Estimates of Early Divergence Times.” *Nature Communications* 5
914 (September): 4956.
- 915 Zhang, Fei, Jinfeng Wu, Nir Sade, Si Wu, Aiman Egbaria, Alisdair R. Fernie, Jianbing Yan, et al. 2021. “Genomic Basis
916 Underlying the Metabolome-Mediated Drought Adaptation of Maize.” *Genome Biology* 22 (1): 260.

917

918

919

920

921

922

923

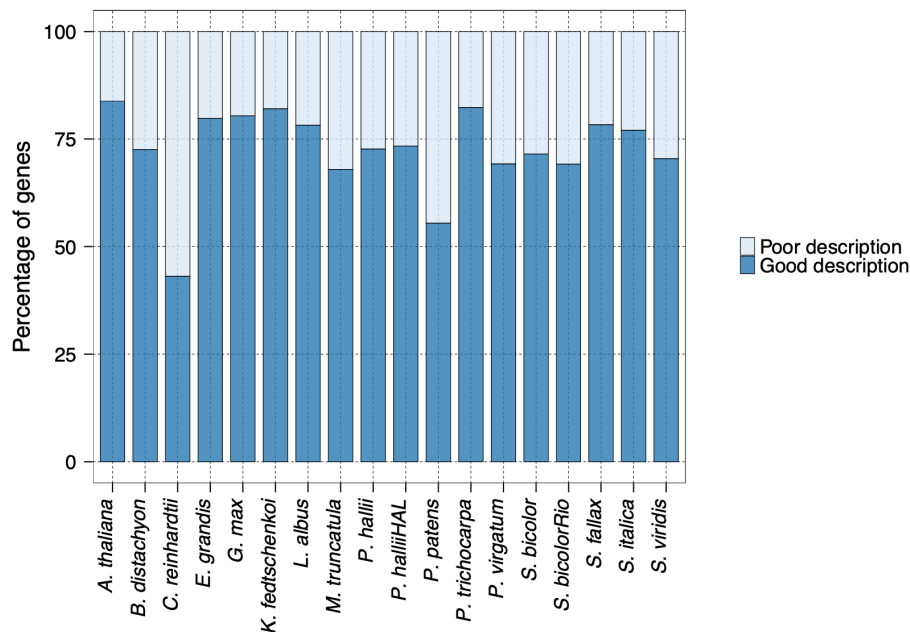
924

925

926

SUPPLEMENTAL FIGURES

927



928

929

930

Supplemental Figure 1 | Classification of gene function descriptions. Percentage of genes with poor and good function descriptions categorized using an augmented dictionary lookup approach that incorporates weighting for negative, positive and adversative keywords.

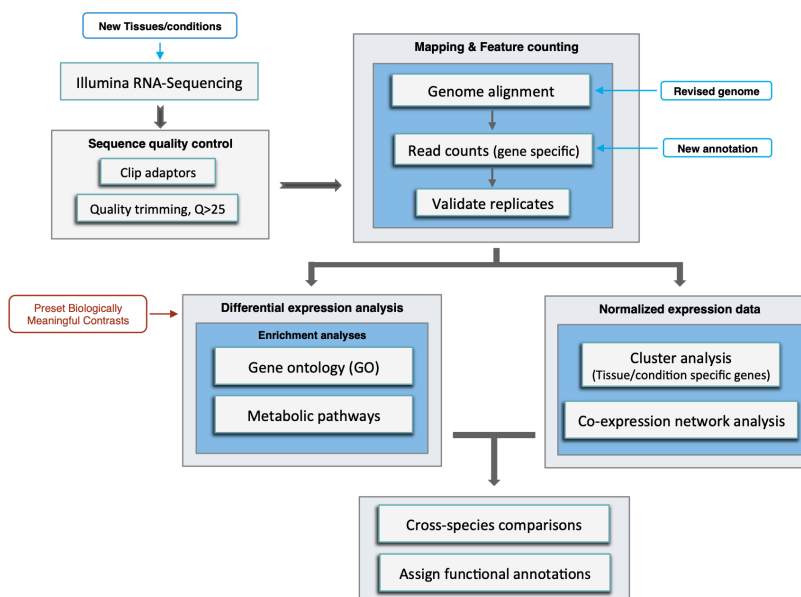
931

932

933

934

935



936

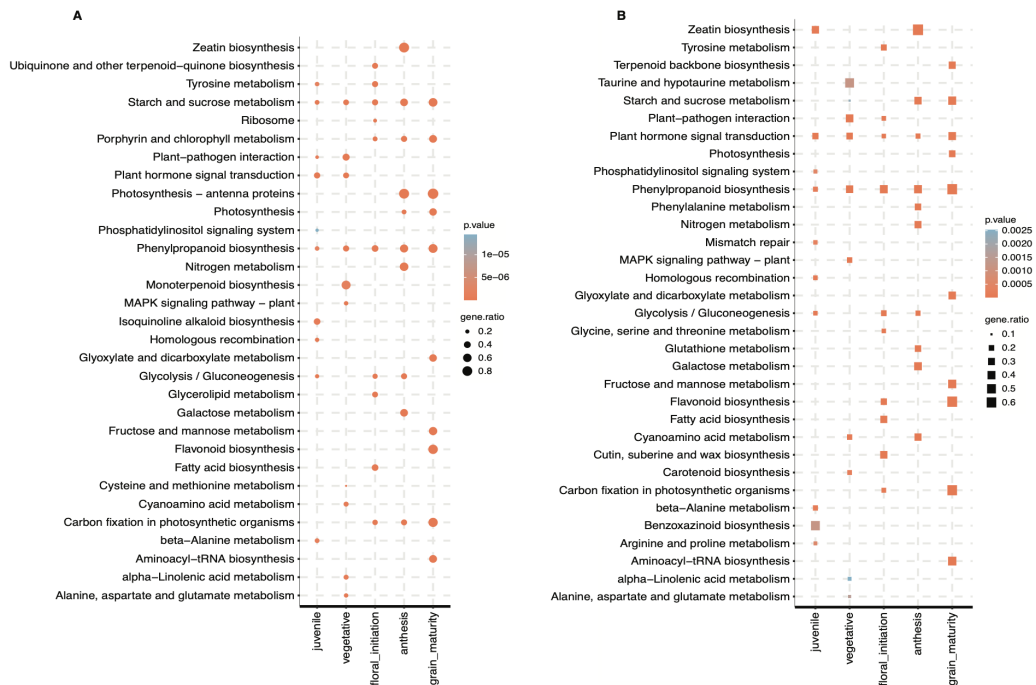
937

Supplemental Figure 2 | Plant Gene Atlas analysis flowchart. Pipeline representing methodology used to analyze RNA-seq data and assign experimentally derived functional annotations.

938

939

940



941

942

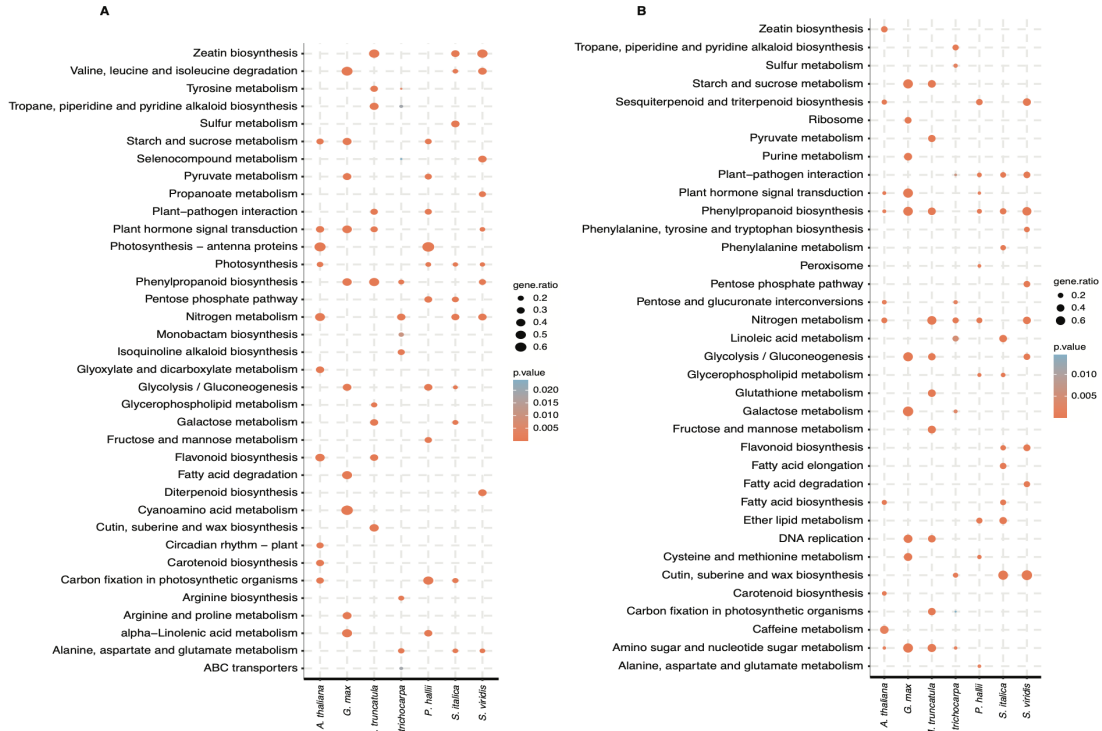
Supplemental Figure 3 | Differentially expressed gene comparison across five developmental stages in *Sorghum*

bicolor. Top 10 KEGG metabolic pathway enrichments ($P < .05$, hypergeometric test) of down-regulated differentially expressed genes in each of the five developmental stages (A) and down-regulated genes unique to each stage (B). 'gene.ratio' represents the ratio of number of DEGs over the number of genes annotated specific to the pathway.

944

945

946



947

948

Supplemental Figure 4 | Transcriptional response of Gene Atlas plants towards NH_4^+ and NO_3^- as the sole nitrogen

source in root tissues. Top 10 KEGG metabolic pathway enrichments ($P < .05$, hypergeometric test) in up-regulated (A) and

949

Sreedasyam et al. 2022 (preprint) JGI Plant Gene Atlas

950 down-regulated (B) differentially expressed genes in roots from Gene Atlas plants in ammonia vs. nitrate comparison. 'gene.ratio'
951 represents the ratio of number of DEGs over the number of genes annotated specific to the pathway.